Black hole mass estimates from high-ionization lines: breaking a taboo?

Paola Marziani[1]

in collaboration with

D. Dultzin[3], A. Negrete[3], A. del Olmo[2], M. A. Martínez-Carballo[2], M. L. Martínez-Aldama[2], G. M. Stirpe[4], E. Bon[5], N. Bon[5], M. D'Onofrio[6]

[1]INAF - Osservatorio Astronomico di Padova, Padova, Italia
[2]Instituto de Astrofísica de Andalucía (CSIC), Granada, España
[3]Instituto de Astronomía, UNAM, México, D.F., México
[4]INAF - Osservatorio Astronomico di Bologna, Bologna, Italia
[5]Astronomska Opservatorija, Beograd, Serbia
[6]Dipartimento di Fisica ed Astronomia "Galileo Galilei", U. di Padova, Padova, Italia

Summary

Introduction: importance of black hole mass estimates

Black hole mass (M_{BH}) estimates: the virial assumption

The “rehabilitating” power of E1

Virial broadening estimators from:

a) Low ionization lines (LILs, IP < 15 eV: Hβ, MgII 2800)

b) High ionization lines (HILs, IP > 40 eV: CIVλ1549)

c) Intermediate ionization lines (IILs: SiIII]λ1892, Al IIIλ1860); preliminary results

“Photoionization masses”

Conclusion

Importance of black hole mass determination

Feedback to the host galaxy: massive, fast outflows are affected by the ratio of radiation to gravitational forces, and are invoked to account for the M_{BH} - bulge velocity dispersion correlation

Fabian 2012; Kormendy & Richstone 2013: King & Pounds 2015, Ferland et al. 2009; Marziani et al. 2016a,b; 2017 (submitted)

The ratio between radiation and gravitation forces: influences **broad-line region dynamics**; lower column density material may flow out of the emitting region

Ferland et al. 2009; Marziani et al. 2010; Netzer & Marziani 2010; Marziani et al. 2017, submitted.

Black hole masses of high redshift quasars provide constraints on primordial black holes collapse

Smith, Broom, Loeb 2017, and references therein; Trakhtenbrot et al. 2015

$$M_{\rm BH} = \frac{f r (\delta v)^2}{G}$$

geometry dynamics

$r_{\rm BLR}$

FWHM
σ
FWZI

f structure factor

$$\text{if } \delta v = \text{FWHM}, \text{isotropy}: \frac{\sqrt{3}}{2}\text{FWHM} \rightarrow f = 0.75$$

δv : virial broadening

estimators from line width measurements

Key assumption: emission line (or component) symmetric and unshifted with respect to the quasar rest frame

Emitting region distance $r_{\rm BLR}$

from central continuum source

Time lag τ given by the peak or centroid of the cross-correlation function between line and continuum ($r_{\rm BLR} = c\,\tau$); scaling laws, or photoionization estimates

Virial black hole masses: scaling laws for large samples

r_{BLR} primary: $r_{BLR} = c\,\tau_{H\beta}$
from Hβ reverberation mapping:
available for ~100 mainly low-z (<1),
type 1 AGN (e.g., Kaspi et al., Bentz. et al. 2009, Du et al. 2016)

r_{BLR} secondary: scaling laws for large samples: $r \propto L^a$, $a \approx 0.5$
(Kaspi et al. 2000; Bentz et al. 2006)

Mass scaling laws:

$M_{BH} = M_{BH}(L, \mathrm{FWHM})$

$M_{BH} = kL^a FWHM^b$

$a \approx 0.5$, $b \approx 2$ (virial)
(e.g., Vestergaard & Peterson 2006; Trakhtenbrot & Netzer 2012)

$a \neq 0.5$, $b \neq 2$
(e.g., Shen & Liu 2012; Park et al. 2013; Shen et al 2016)

$$\text{Eddington ratio} = \frac{L_{\rm bol}}{L_{\rm Edd}} \propto \frac{\lambda L_\lambda \times \text{B.C.}}{M_{\rm BH}}$$

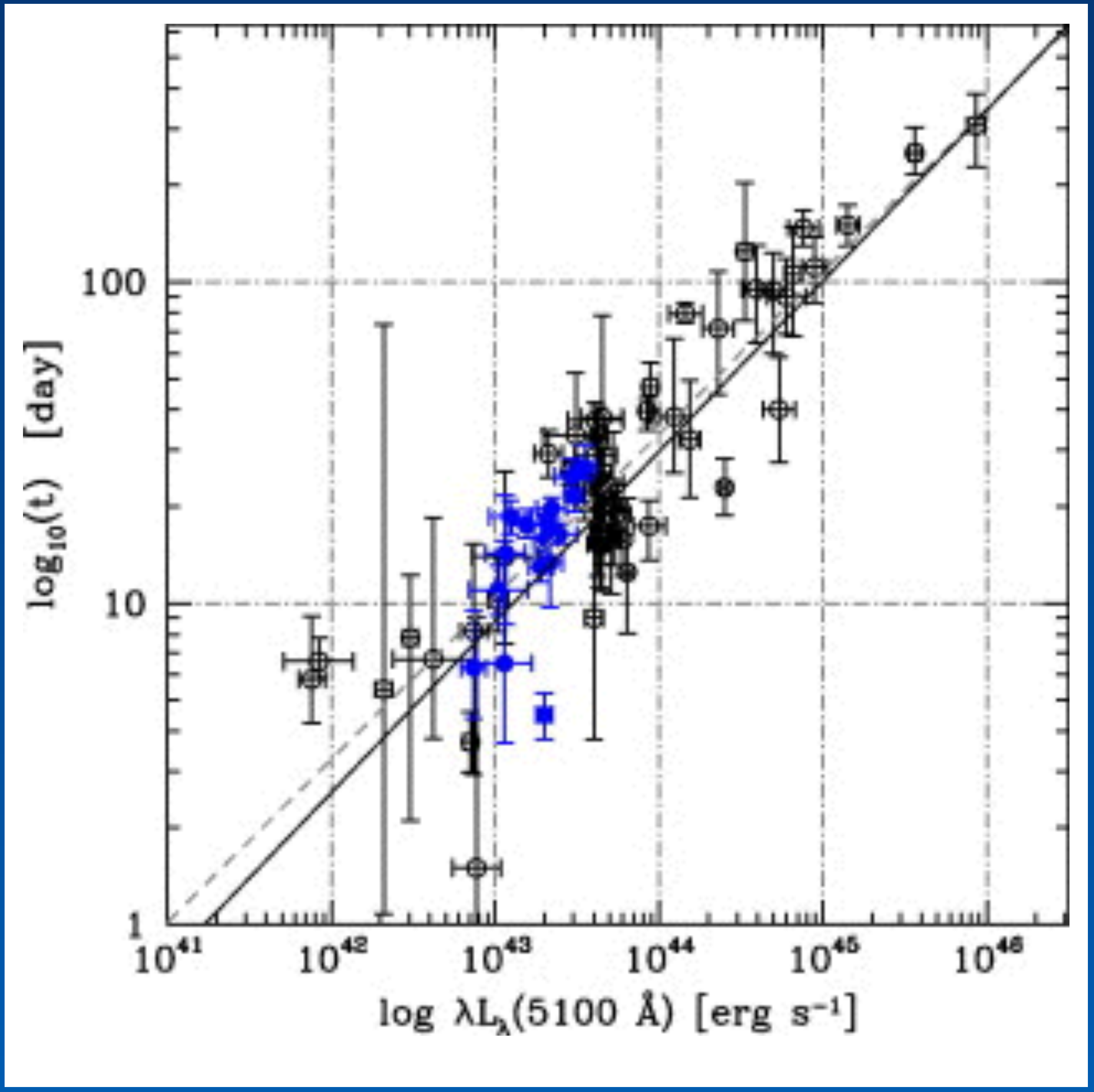

The M_{BH} scaling laws provides a simple recipe usable with single epoch spectra

Caveats

Reverberation mapping assumptions compact continuum source, fairly linear response.
Unpredicted behavior of NGC 5548 in 2014: shielding, optically thin gas, changing size of continuum source?

Horne et al. 2017; Pei et al. 2017; Fasnaugh et al 2016

The **r_{BLR} - L scaling relation**: has a non-negligible intrinsic dispersion, and r_{BLR} depends on dimensionless accretion rate.

Du et al. 2016; 2017

Line profiles as virial broadening estimators: errors so large to lead to full loss of information

e.g., Croom 2011

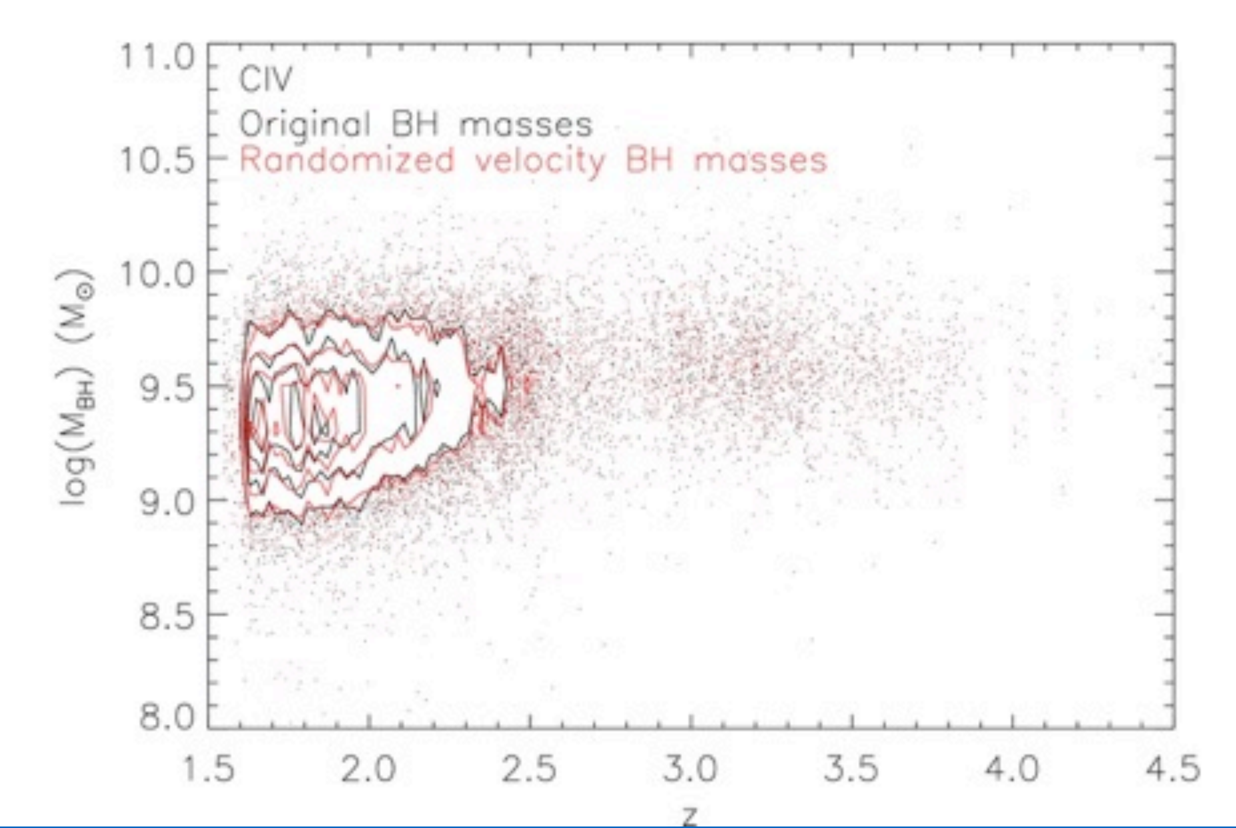

One value of the structure factor obtained scaling the M_{BH} to agree with the dynamical masses, f(FWHM)≈2 but structure factor likely different for different type-1 quasar populations.

Woo et al. 2010; cf Gültekin et al. 2009;
Onken et al. 2004;
Ferrarere & Merritt 2000;
also Graham et al. 2011

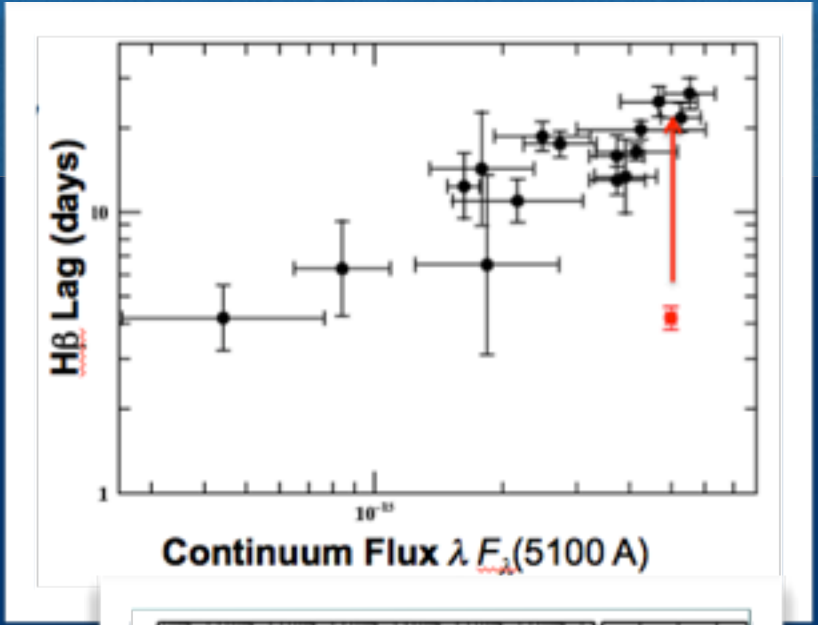

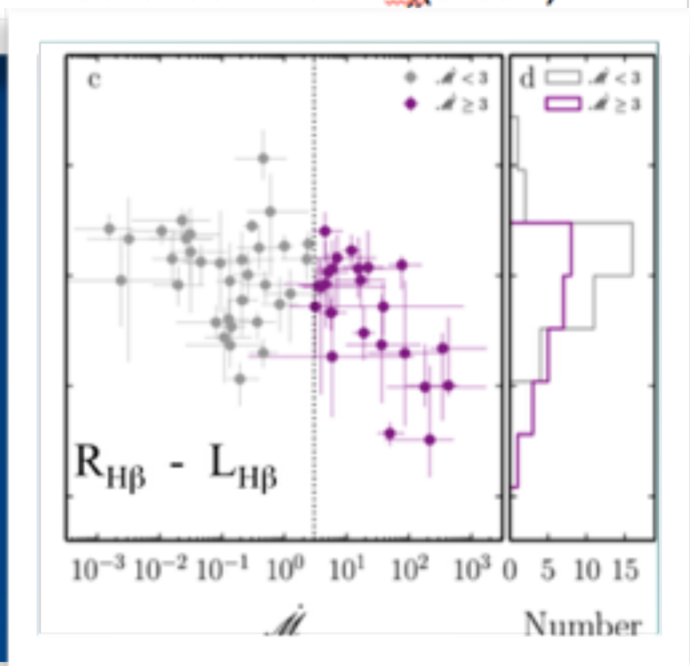

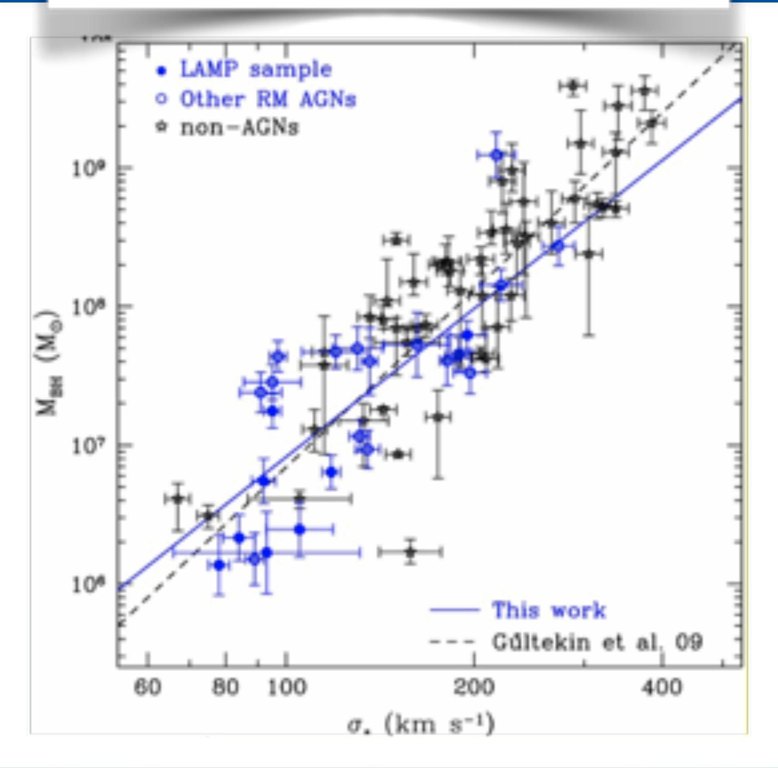

Eigenvector 1: an useful tool to organize quasar diversity

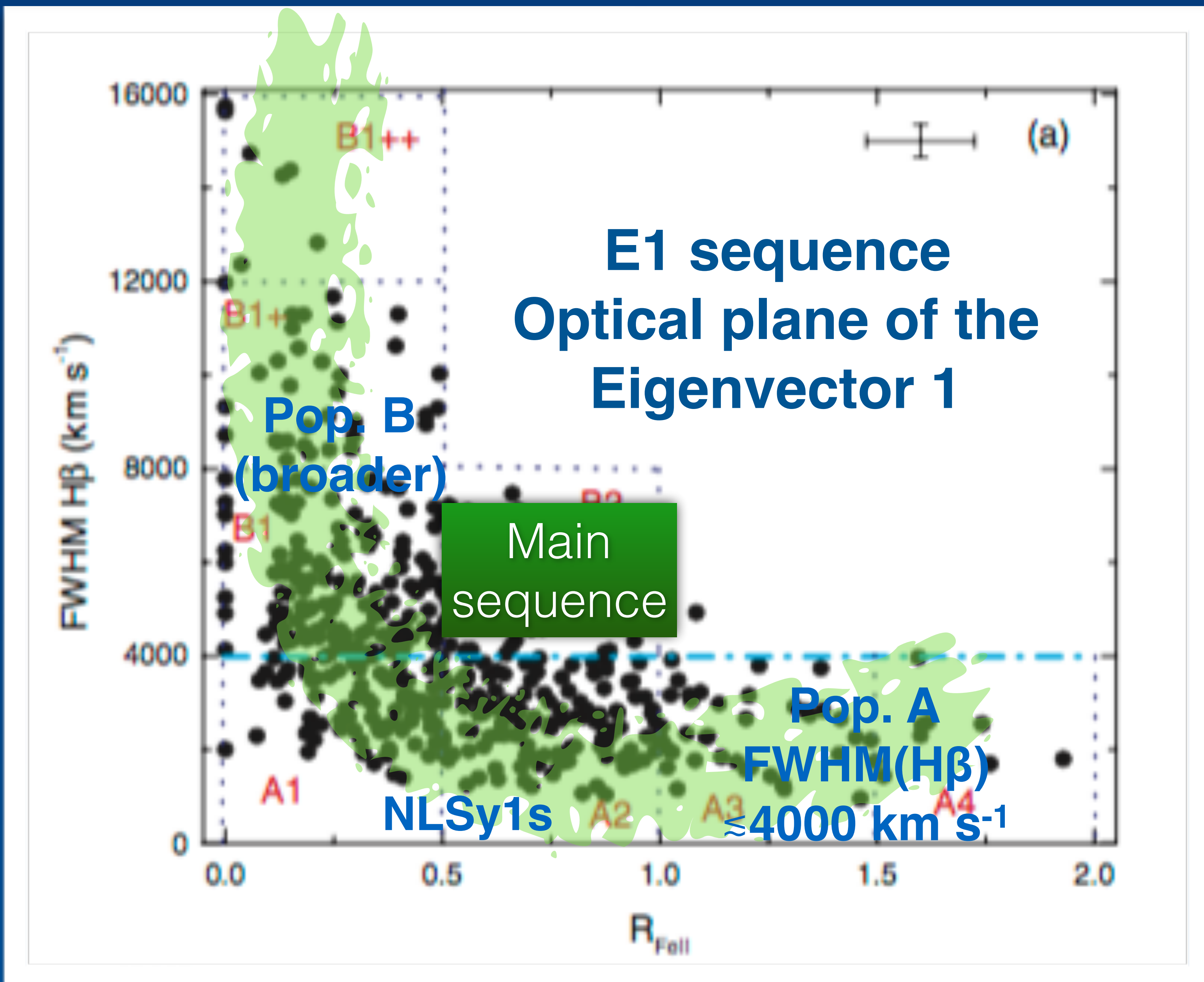

Sulentic et al. 2002 ($z < 1$, log L < 47 [erg/s]); **Boroson & Green 1992; Sulentic et al. 2000**, 2007;   discussed in more than 400 papers: Dultzin-Hacyan et al. 1997;   Shang et al. 2003, Yip et al.2004, Kruzcek et al 2011; Tang et al. 2012; Kuraszkiewicz et al. 2008; Mao et al. 2009; Grupe 2004, Wang et al. 2006 SDSS data : Richards et al. 2011; Shen & Ho 2014, Sun & Ho 2015, Brotherton et al. 2015

Eigenvector 1: Originally defined by a Principal Component Analysis of PG quasars, and associated with an anti-correlation between strength of FeIIλ4570, R_{FeII} (or [OIII] 5007 peak intensity) and   FWHM of Hβ.

The **E1 main sequence (MS) in the optical plane** FWHM(Hβ) vs R_{FeII} = I(FeIIλ4570)/I(Hβ) allows for the **definition of spectral types.**

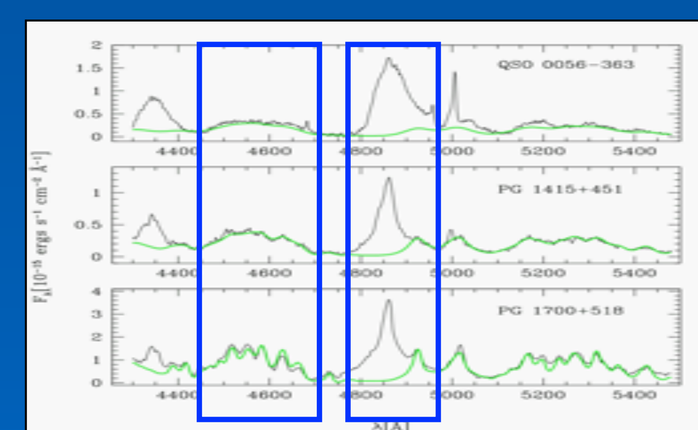

$$R_{\rm FeII} = \frac{I({\rm FeII}\lambda 4570)}{I(H\beta)} \approx \frac{W({\rm FeII}\lambda 4570)}{W(H\beta)}$$

The “rehabilitating power of Eigenvector 1”: two Populations, A and B

L/L_{Edd} is the driver of the E1 MS

Boroson & Green 1992, Marziani et al. 2001, Shen &Ho 2014, Sun & HSen 2015

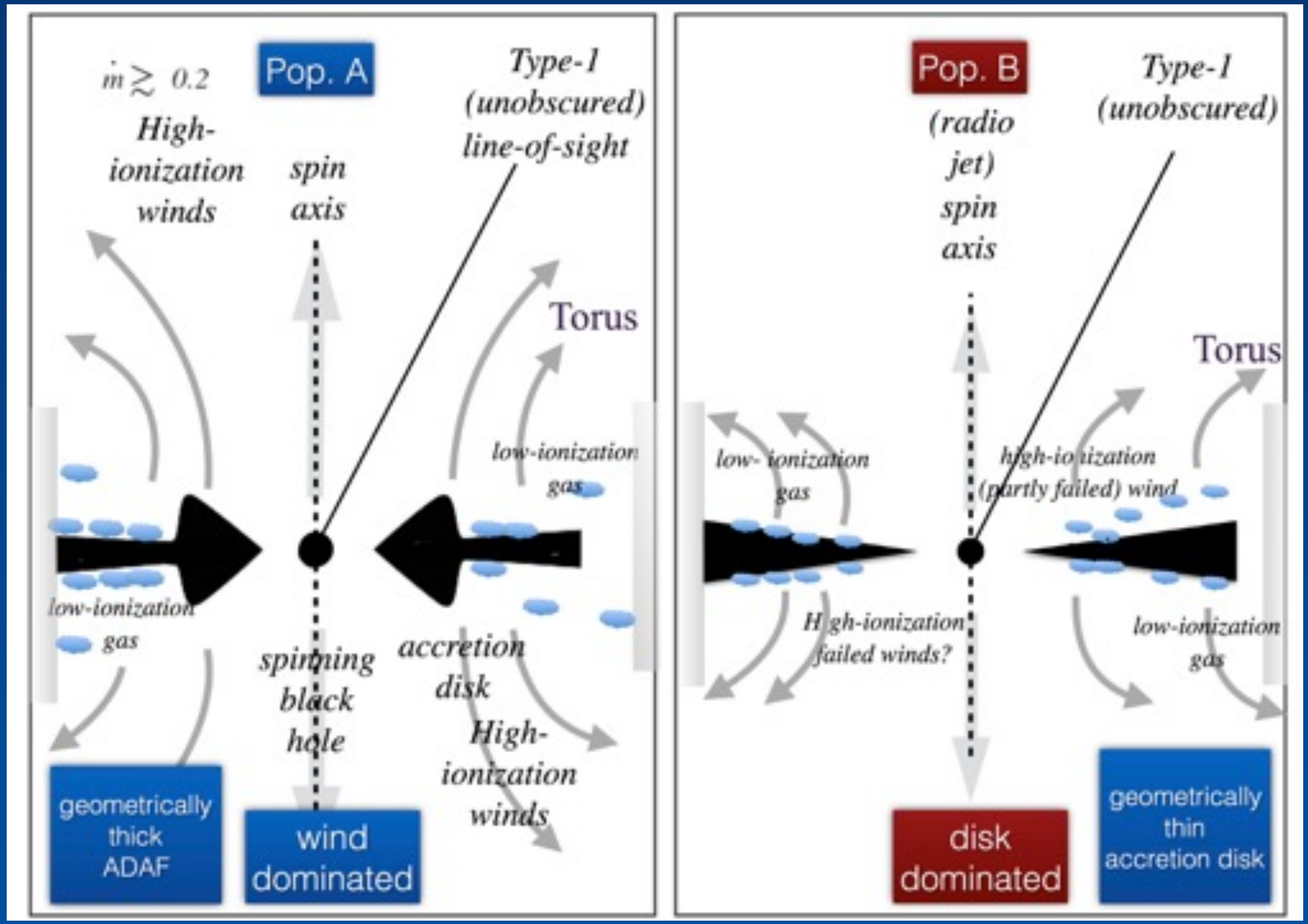

Population A (FWHM Hβ<4000 km/s) and Population B(roader) sources

Pop. A: high L/L_{EDD}; Pop. B: low L/L_{EDD}.

More appropriate than the distinction NLSy1-rest of type-1 AGNs; called wind and disk dominated by Richards et al., Population 1 and 2 by Collin et al. 2006.

Probably due to a change of accretion mode

Marziani et al. 2003b, Marziani et al. 2014

4DE1: 2 more “ortogonal” parameters: Γ_{soft}, c(½) CIVλ1549;

many more correlates, including line profile shapes

Table 1s of Sulentic et al. 2011 and Fraix-Burnet et al. 2017

The 4D Eigenvector 1 space of quasars

Observed parameter	Physical interpretation
R_{FeII}=I(FeII)/I(Hβ)	ionization degree *col. density, Z*
FWHM(Hβ)	velocity field of low-ionization gas
CIVλ1549 Shift	velocity field of high-ionization gas
Γ_{soft} (0.2-2 KeV)	Compton thick / accretion disk emission?

} Optical plane of 4DE1 (first two rows)

Virial broadening estimators: LILs along E1 sequence

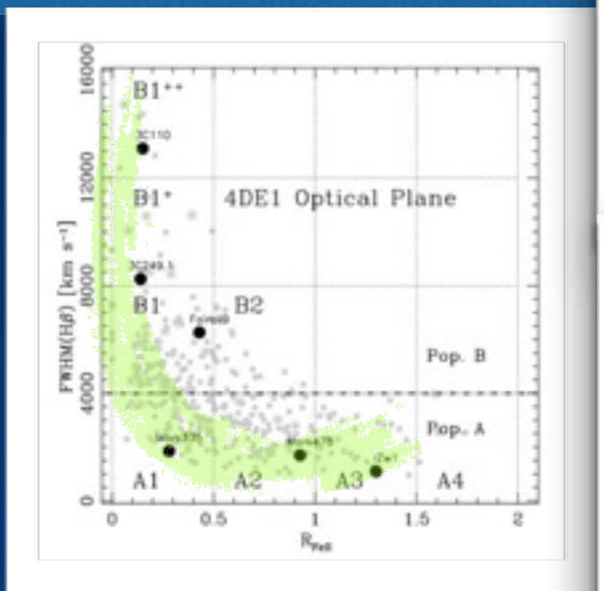

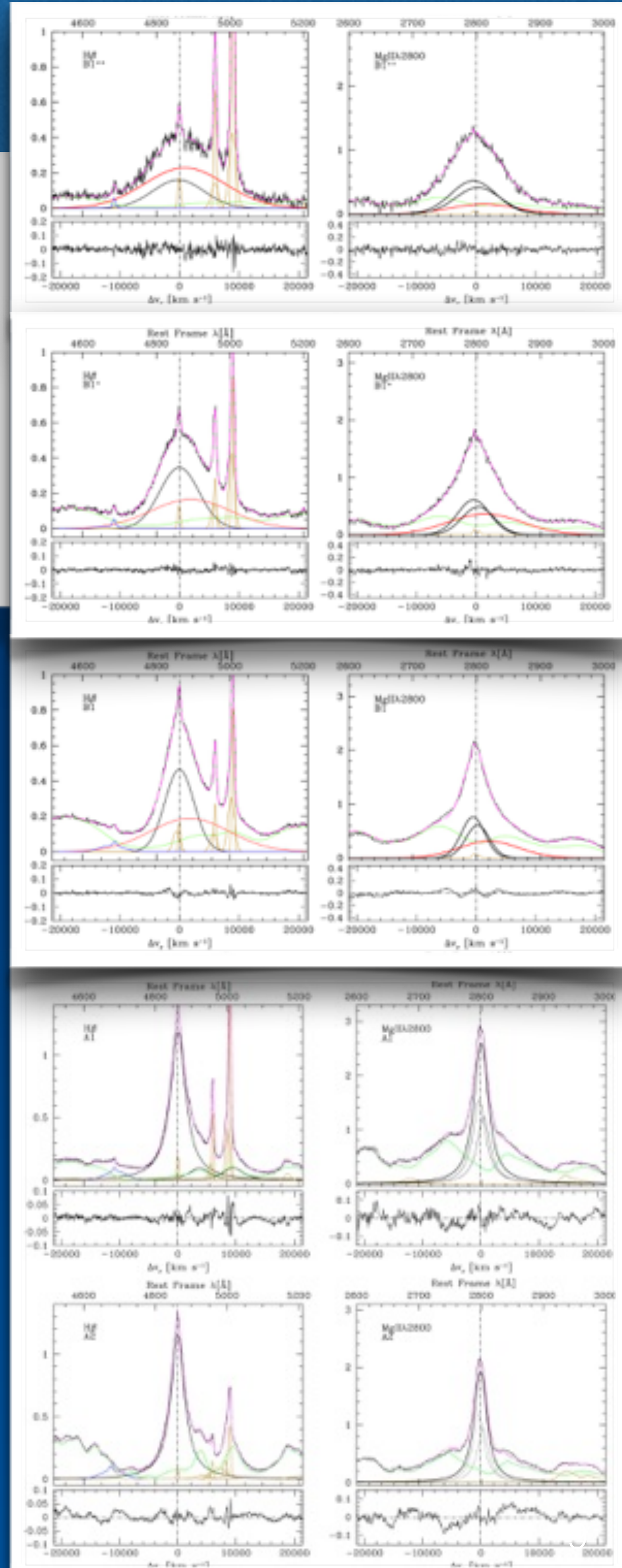

Hβ and MgII

from **extreme Pop. B**: low FeII, broad profiles

redward asymmetric

Broad component + (redshifted) very-broad component

to **extreme Pop. A,** narrower, strong FeII, slightly blueward asymmetric

Lorentzian profiles + blueshifted excess

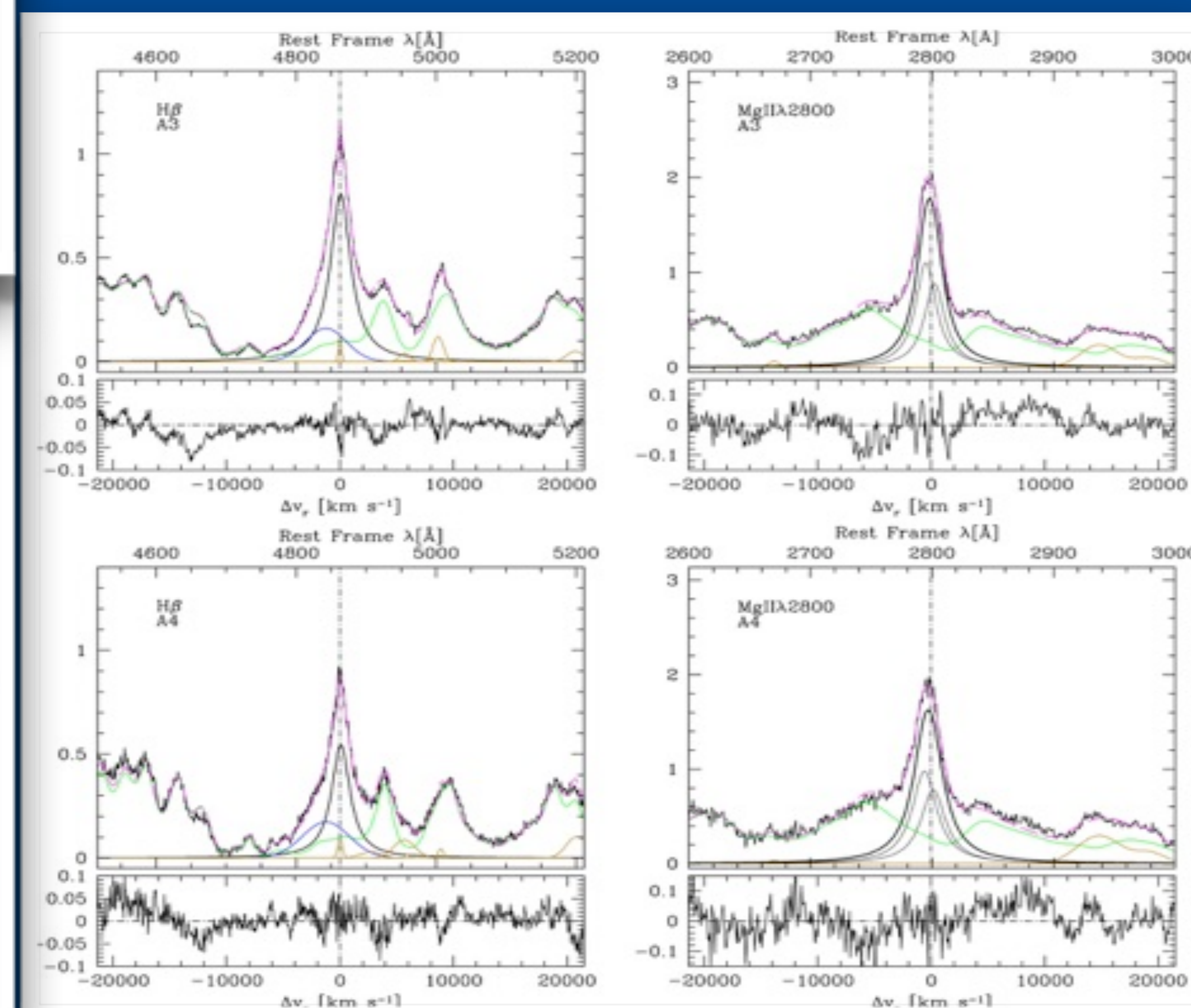

Marziani et al 2013a,b; SDSS sample covering both Hβ and MgII 0 .4 < z < 0.7

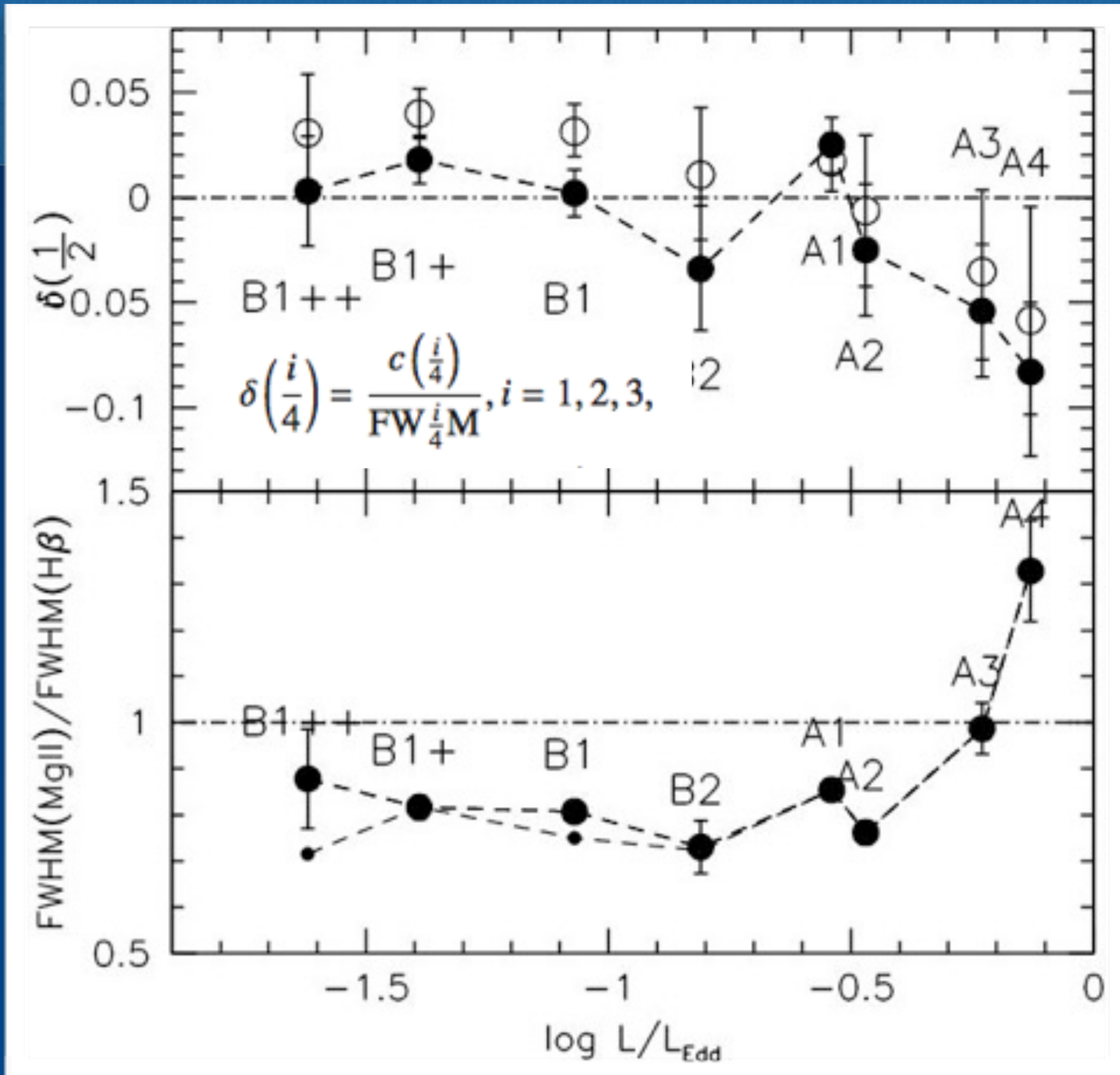

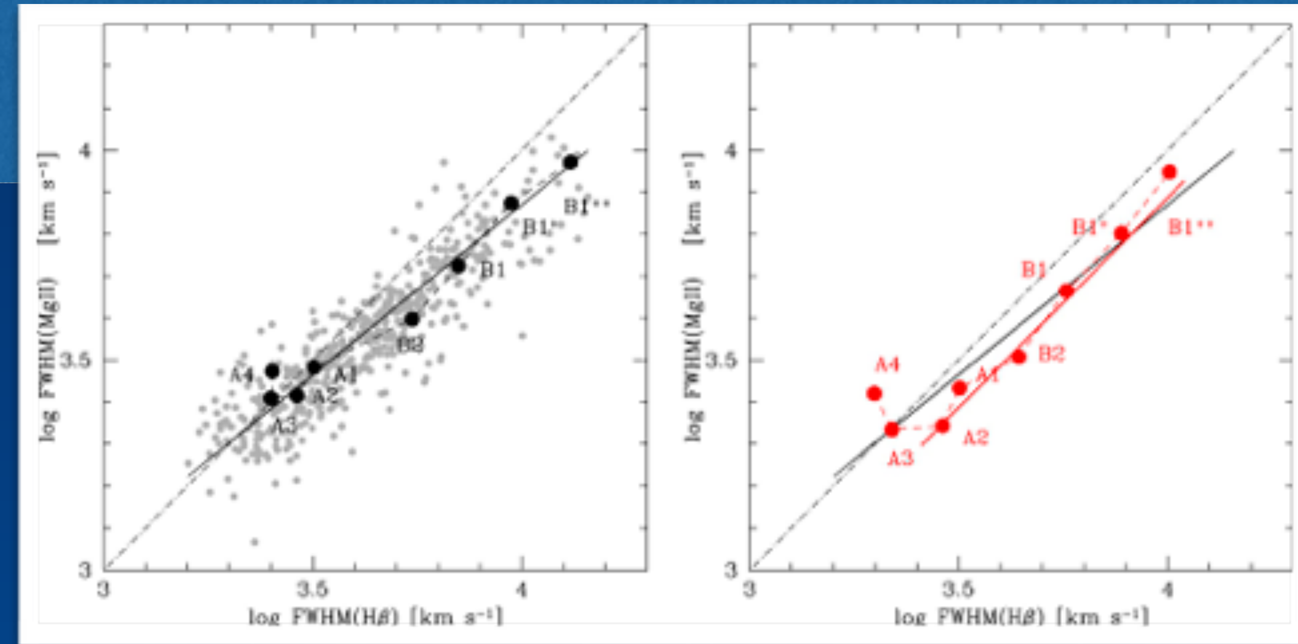

SDSS sample covering both Hβ and MgII 0 .4 < z <0.7; Marziani et al. 2013a,b; Wang et al. 2009; cf. Trakhtenbrot & Netzer 2012; Mejia-Restrepo et al. 2016

LIL resonance line MgIIλ2800: low ionization outflows detected in the extreme Pop. A spectral types

$$FWHM(\mathrm{line})_{\mathrm{vir}} = \xi FWHM(\mathrm{line})_{\mathrm{obs}}$$

where

$$\xi = \frac{FWHM(\mathrm{line})_{\mathrm{BC}}}{FWHM(\mathrm{line})_{\mathrm{obs}}},$$

LILs are dominated by a symmetric, “virialized” broad component: 1 ≳ ξ ≳ 0.75.

	$\xi_{H\beta}$	ξ_{MgII}
A3-A4	0.8/0.9	0.75/0.8
A1-A2	1.0	1.0
B1	0.8	0.9
$B1^{+}/B1^{++}$	0.8	0.9

Virial broadening estimators: the HIL CIVλ1549 along the E1 sequence

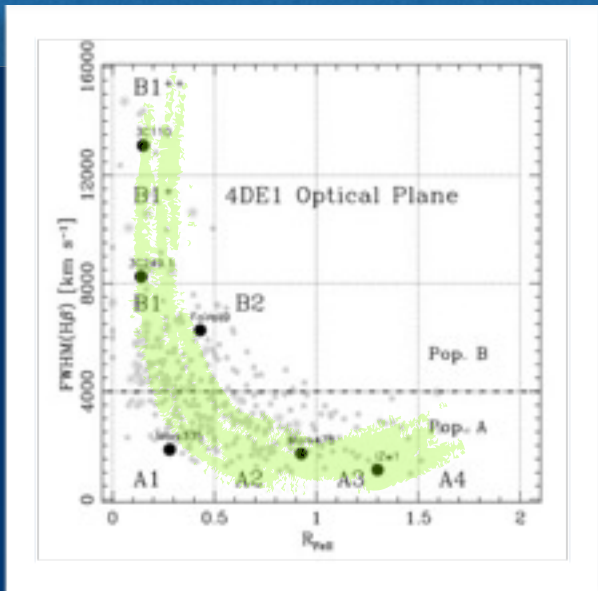

CIVλ1549: scaled Hβ from + excess blueshifted emission increasing from B1++ to A3

almost symmetric, unshifted LIL (⇒“virialized” emitting region) +
outflow/wind component that dominates in A3/A4 spectral types

e.g., Leighly 2000, Bachev et al. 2004, Marziani et al. 2010; Denney et al. 2012

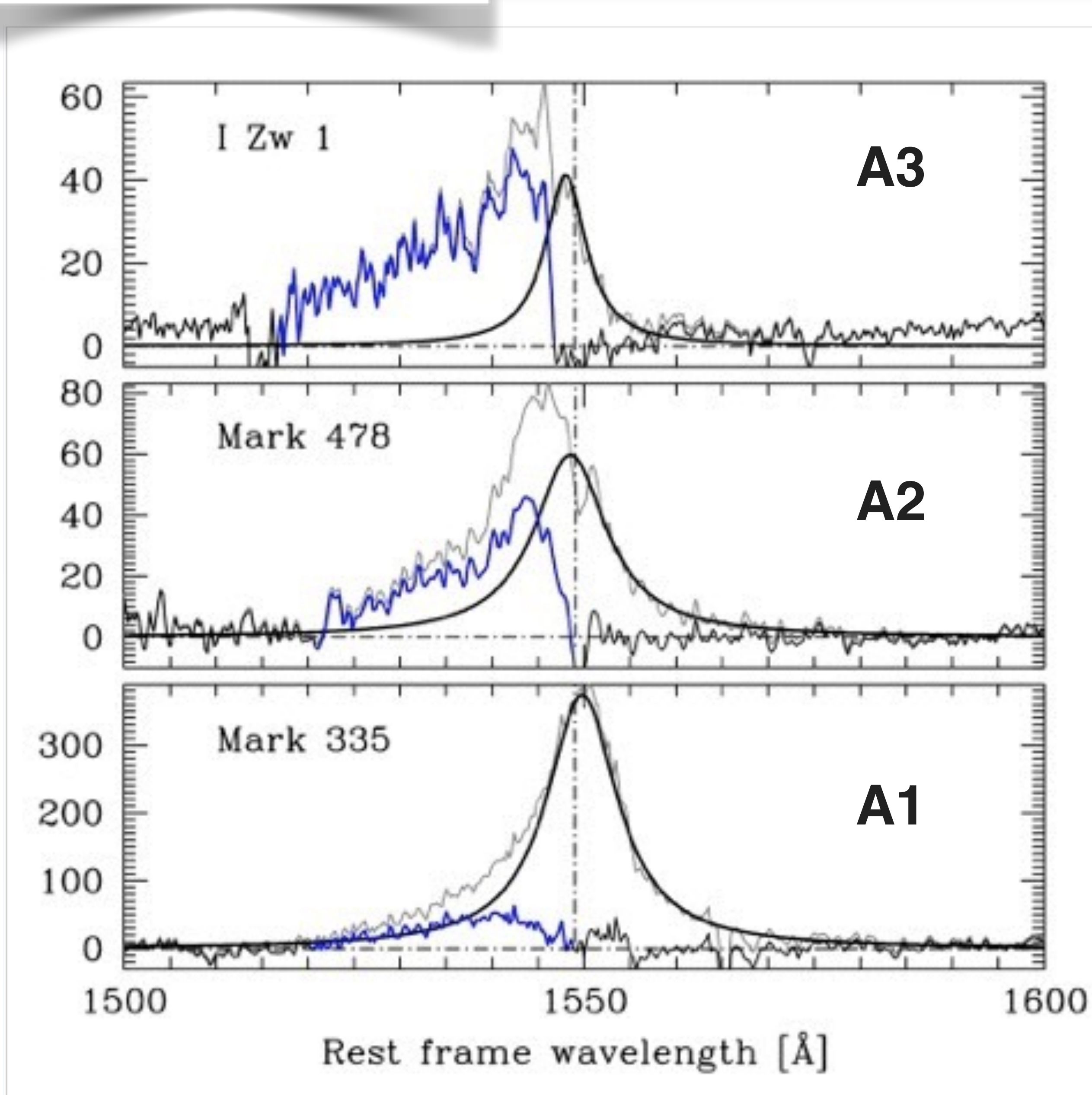

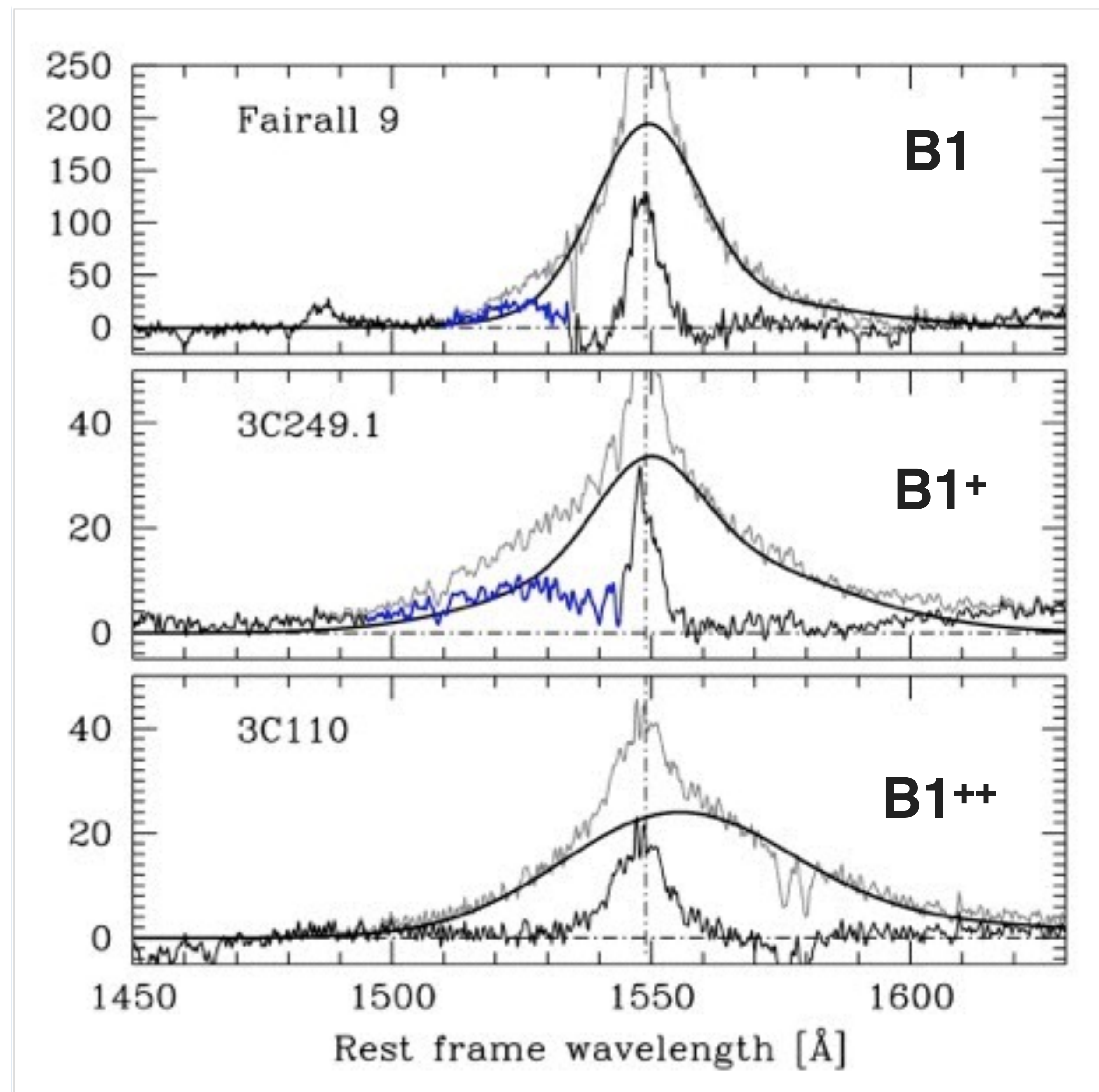

Virial broadening estimators: the HIL CIVλ1549 along the E1 sequence

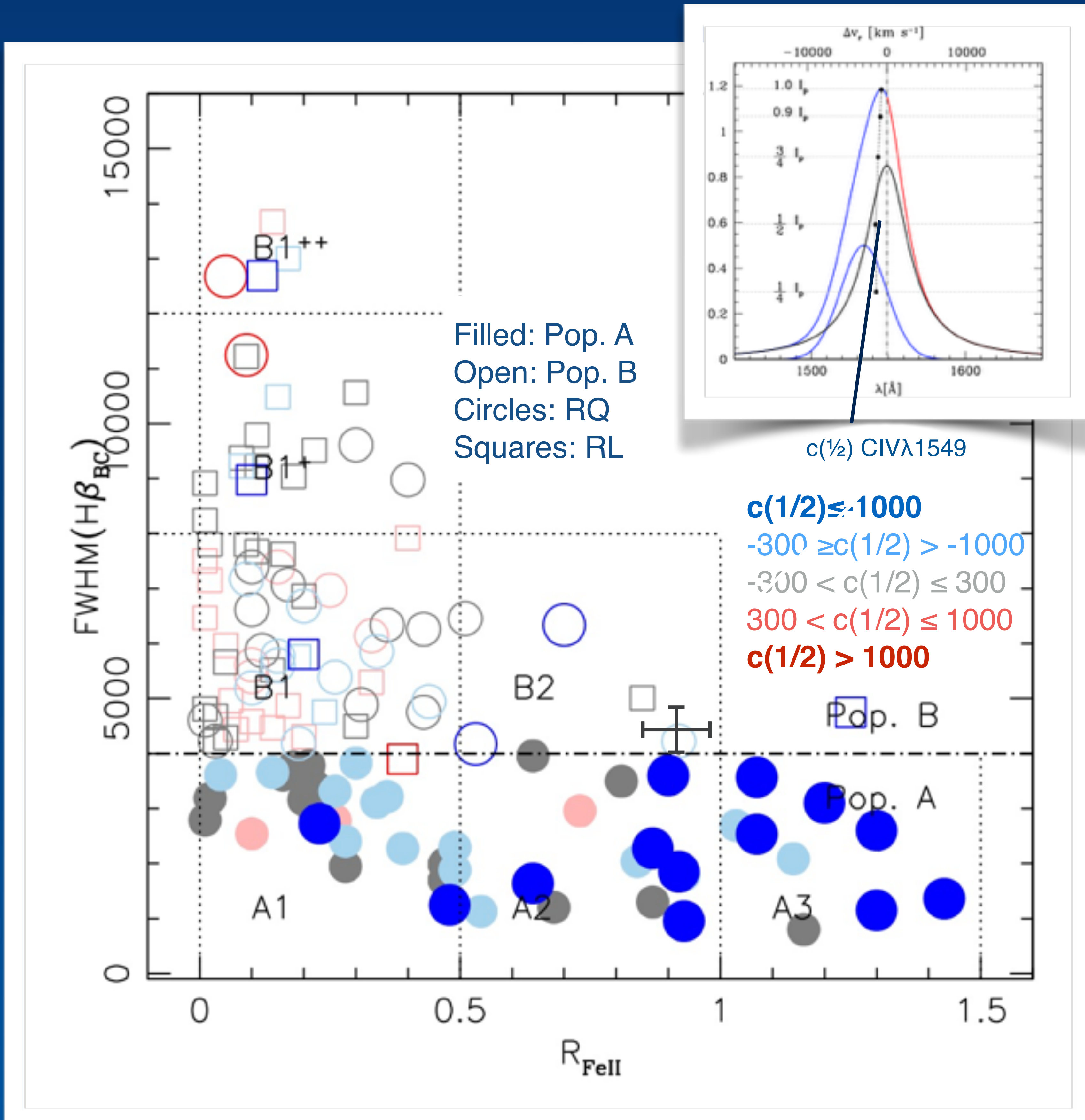

Large shift of CIVλ1549 centroid at ½ along the MS are found for FWHM(Hβ) < 4000 km s^{-1} in the E1 optical plane.

This result also reinforces the suggestion of a discontinuity at FWHM(Hβ) ≈ 4000 km s^{-1} suggested by the Hβ profile shape change.

Marziani & Sulentic 2012; Sulentic et al. 2007; low *z* sample UV FOS data

Virial broadening estimators: the CIVλ1549 “taboo”

1. FWHM(Hβ) and L_λ(5100 Å): For the optical continuum luminosity and FWHM of the Hβ broad component,

$$\log M_{\rm BH}({\rm H}\beta) = \log\left\{\left[\frac{\rm FWHM(H\beta)}{1000\ \rm km\ s^{-1}}\right]^2\left[\frac{\lambda L_\lambda(5100\ \text{Å})}{10^{44}\ \rm ergs\ s^{-1}}\right]^{0.50}\right\} + (6.91 \pm 0.02). \quad (5)$$

$$\log M_{\rm BH}({\rm C\ IV}) = \log\left\{\left[\frac{\rm FWHM(C\ IV)}{1000\ \rm km\ s^{-1}}\right]^2\left[\frac{\lambda L_\lambda(1350\ \text{Å})}{10^{44}\ \rm ergs\ s^{-1}}\right]^{0.53}\right\} + (6.66 \pm 0.01). \quad (7)$$

Vestergaard & Peterson 2006; mass “taboo”: Sulentic et al. 2007; Netzer et al. 2007

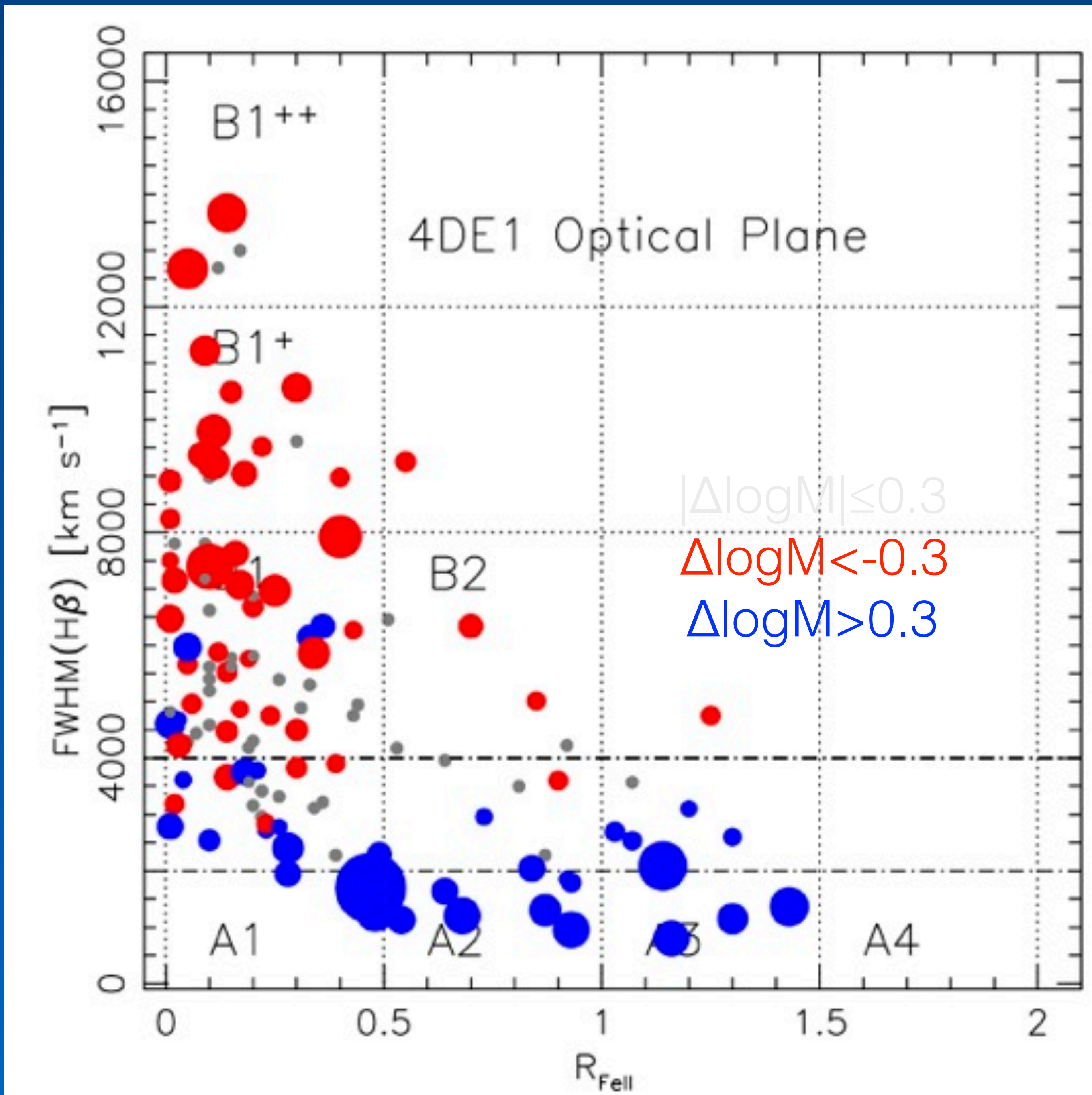

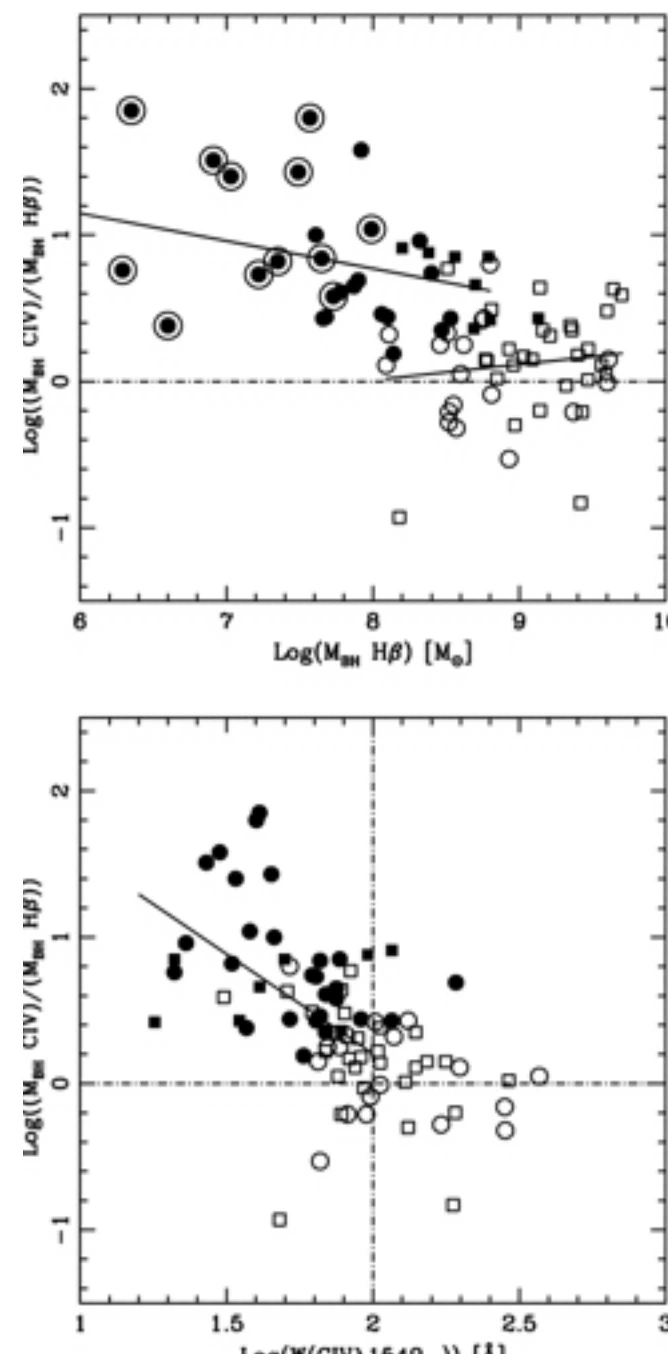

Scaling laws assumed that the width of CIV and Hβ are equivalent

Bias along the E1 sequence, especially for Pop. A

errors as large as 2 dex.

Pop. A sources are more frequently selected at high z, high L

Virial broadening estimators: LIL Hβ behavior over a wide luminosity range

Composite spectra: Hβ becomes broader with increasing *L* (over 43 < logL < 48.5 [erg s^{-1}]) but shapes are similar to the ones at low z

Pop. A Pop. B

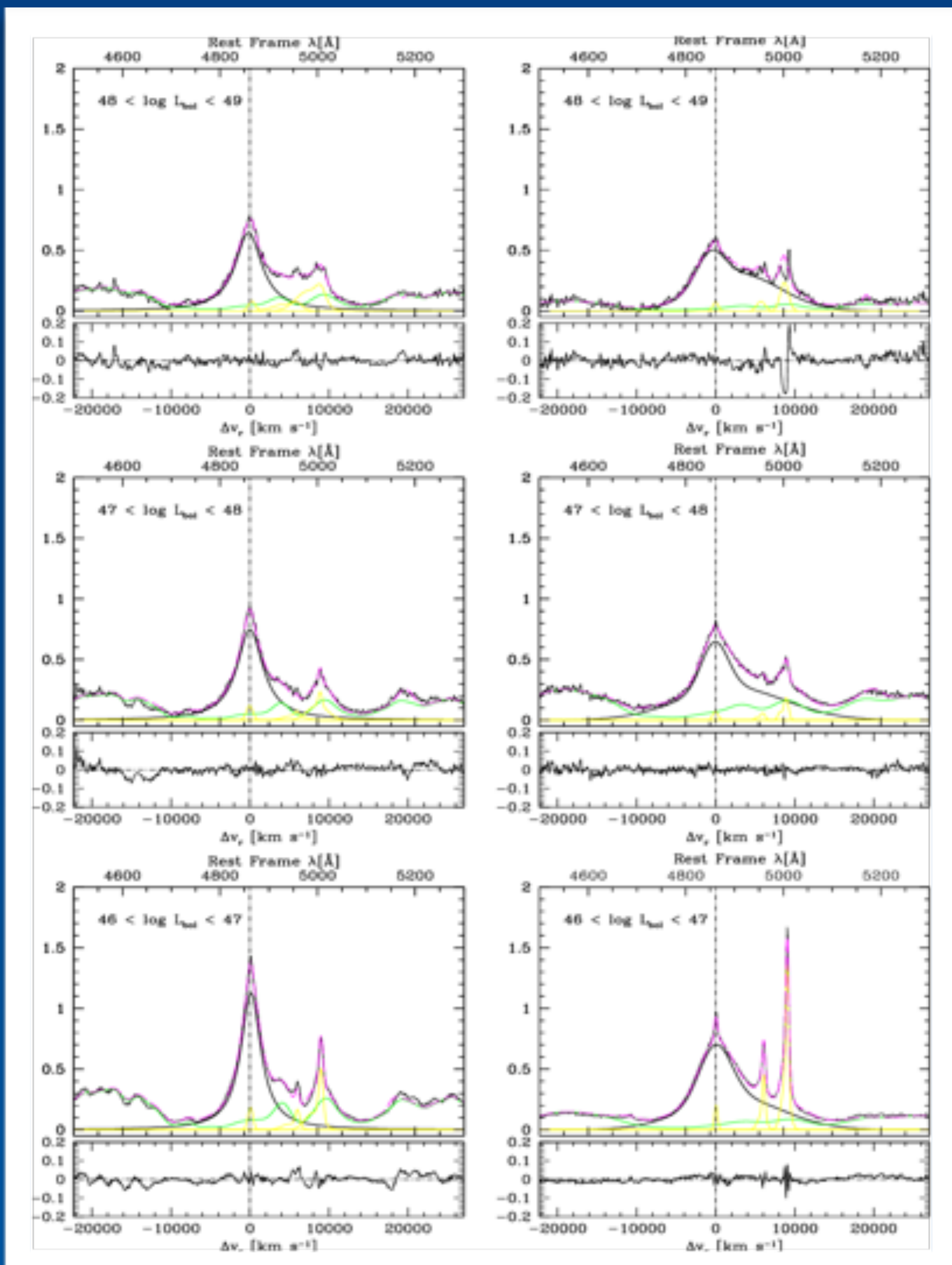

Pop. A Pop. B

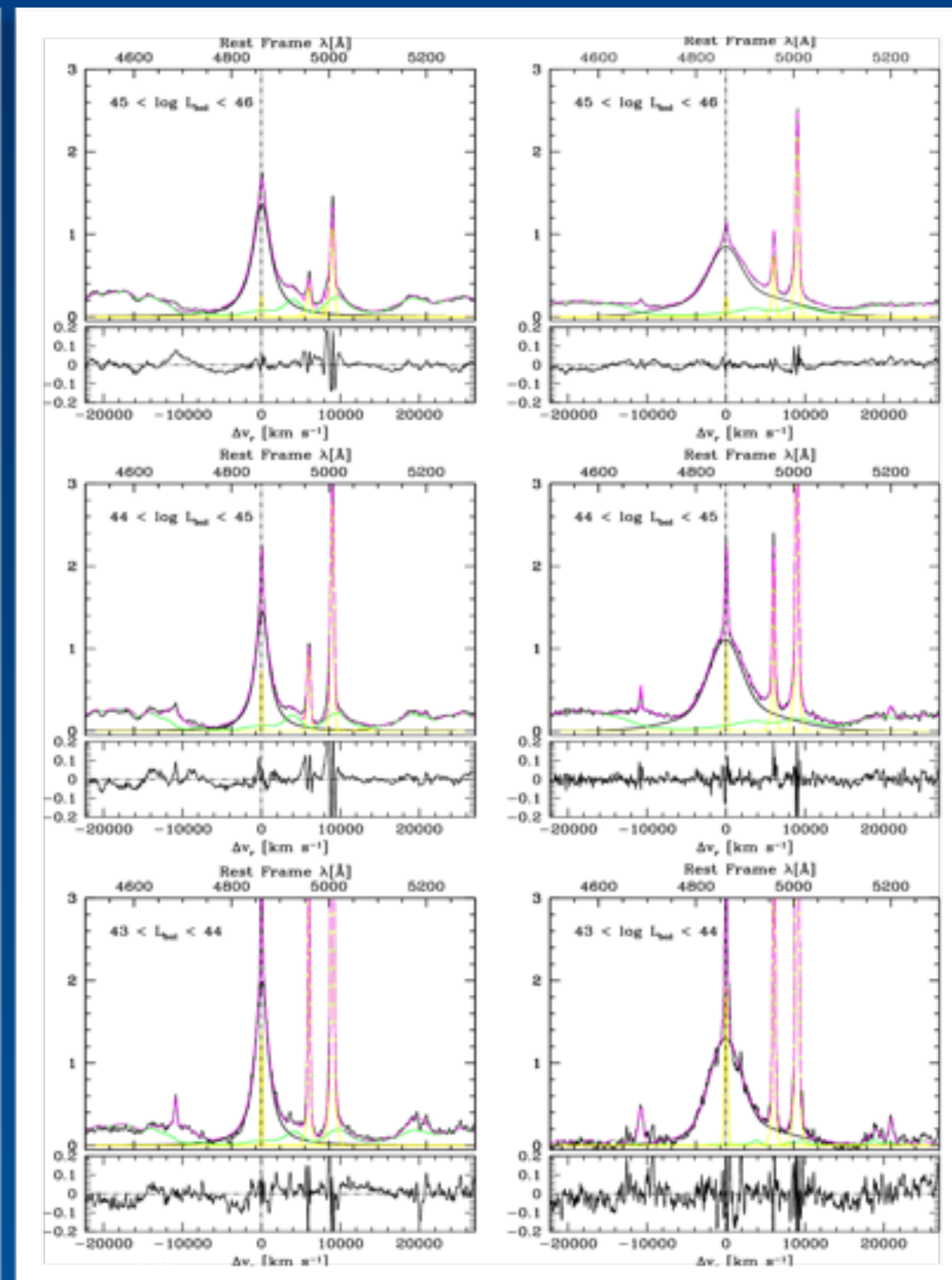

The Pop. A / Pop. B differences are preserved at high L

HE/ISAAC high-L sample (52 sources) + SDSS continuum subtracted spectra

Marziani et al. 2009; Zamfir et al. 2010

Virial broadening estimators: LIL Hβ at high-L

"Symmetrization" methods:

– substitution of the BC extracted through the `specfit` analysis in place of the full Hβ profile.
– symmetrization of the profile: $\mathrm{FWHM_{symm}} = \mathrm{FWHM} - 2\,c(\frac{1}{2})$ (symm in Fig. 2);
– correction based on spectral type, as defined from the analysis of the Hβ profile in a large SDSS-based sample at $0.4 \lesssim z \lesssim 0.7$ (labeled as cm in Fig. 2), following Marziani et al. (2013a). In practice, this means to correct Hβ for Pop. B sources by a factor $\xi_{\mathrm{H}\beta} \approx 0.8$;
– correction derived by pairing the observed FWHM to the best width estimator from reverberation mapping, following the relation $\mathrm{FWHM_c} \approx 1.14\,\mathrm{FWHM} - 601 - 0.0000217\mathrm{FWHM}^2$ derived by Sulentic et al. (2006, labeled `corr`);

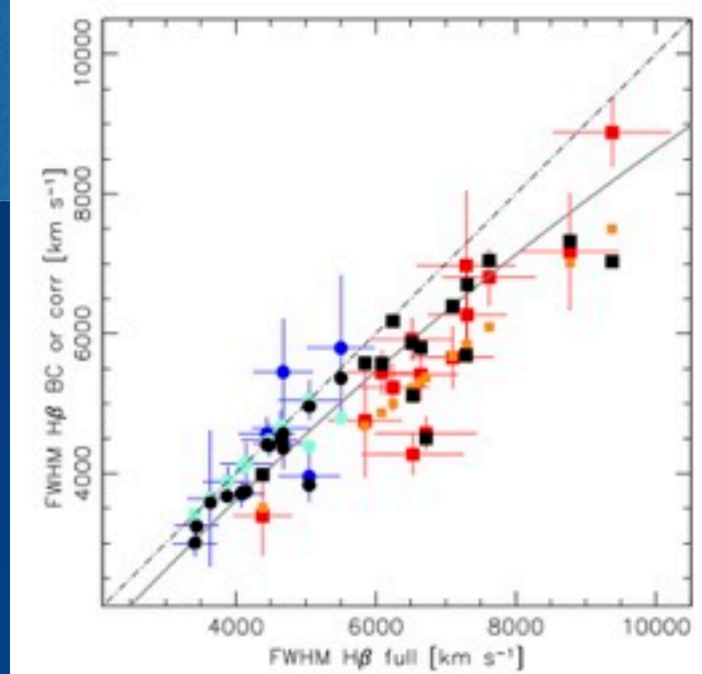

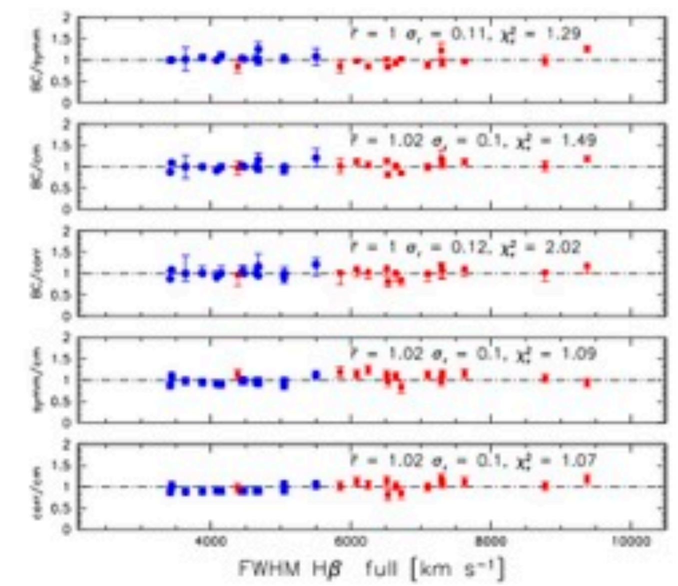

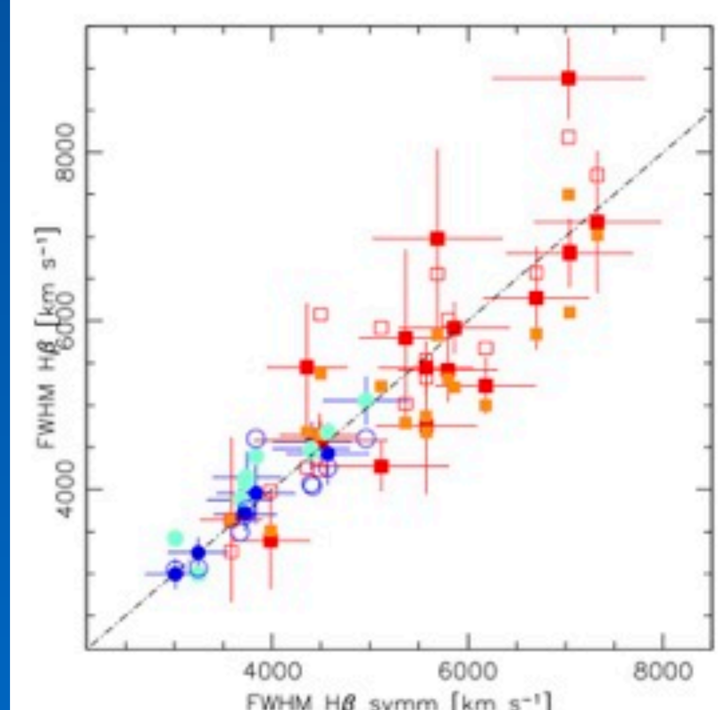

All "symmetrization" methods could be considered equivalent at high L.

The Hβ profile shapes at high L are consistent with those at low-z, lower L.

A "virialized system" emitting mainly LILs

Virial broadening estimators: LIL Hβ behavior over a wide luminosity range

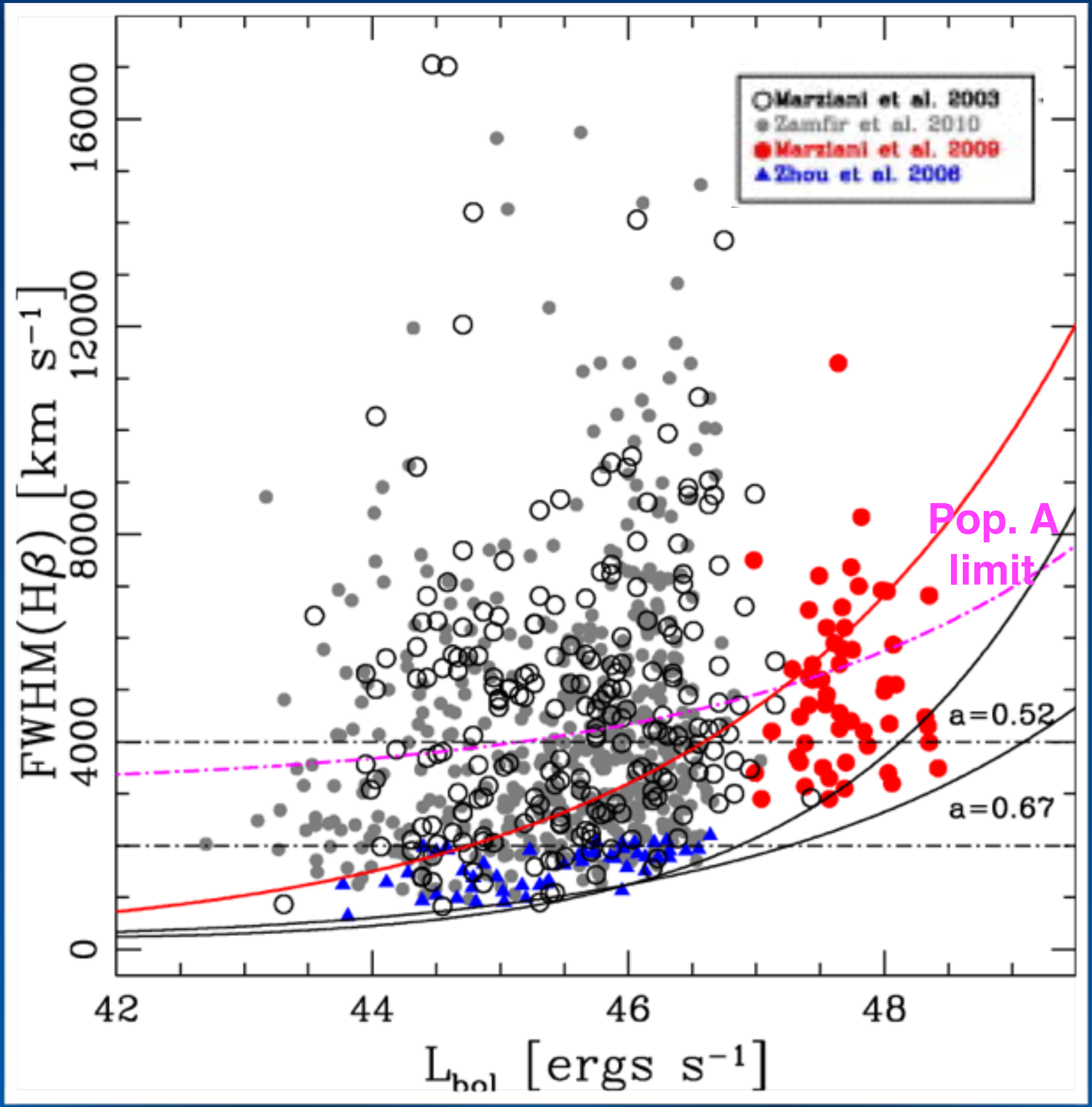

Minimum FWHM(Hβ) is luminosity-dependent, consistent with virial assumption.

The Pop. A limit is also luminosity dependent.

Curves assume the virial relation and r_{BLR} scaling with luminosity:

$r_{BLR} FWHM^2 \propto M$

$r_{BLR} \propto L^a$

$FWHM \propto (L/M)^{-1} L^{((1-2a)/2)}$

Minimum FWHM is obtained for a limiting Eddington ratio ~ 1.

Marziani et al. 2009

Virial broadening estimators: CIVλ1549 at high luminosity

High-L ($\gtrsim 10^{47}$ erg s^{-1}, 1 <z<2) :
VLT/FORS HE sample (Sulentic et al 2017; CIV, 28 objects)
$\cap$
VLT/ISAAC HE sample (Marziani et al. 2009, 52 objects)

median 3000 km s^{-1} for Pop. A; 2 cases with CIV c(1/2) blueshift amplitude larger than 5000 km s^{-1}

Widespread powerful outflows coexisting with a virialized low-ionization component

L>10^{47} erg s^{-1}: high amplitude CIV 1549 blueshifts in both Pop. A and B

Sulentic et al., 2017

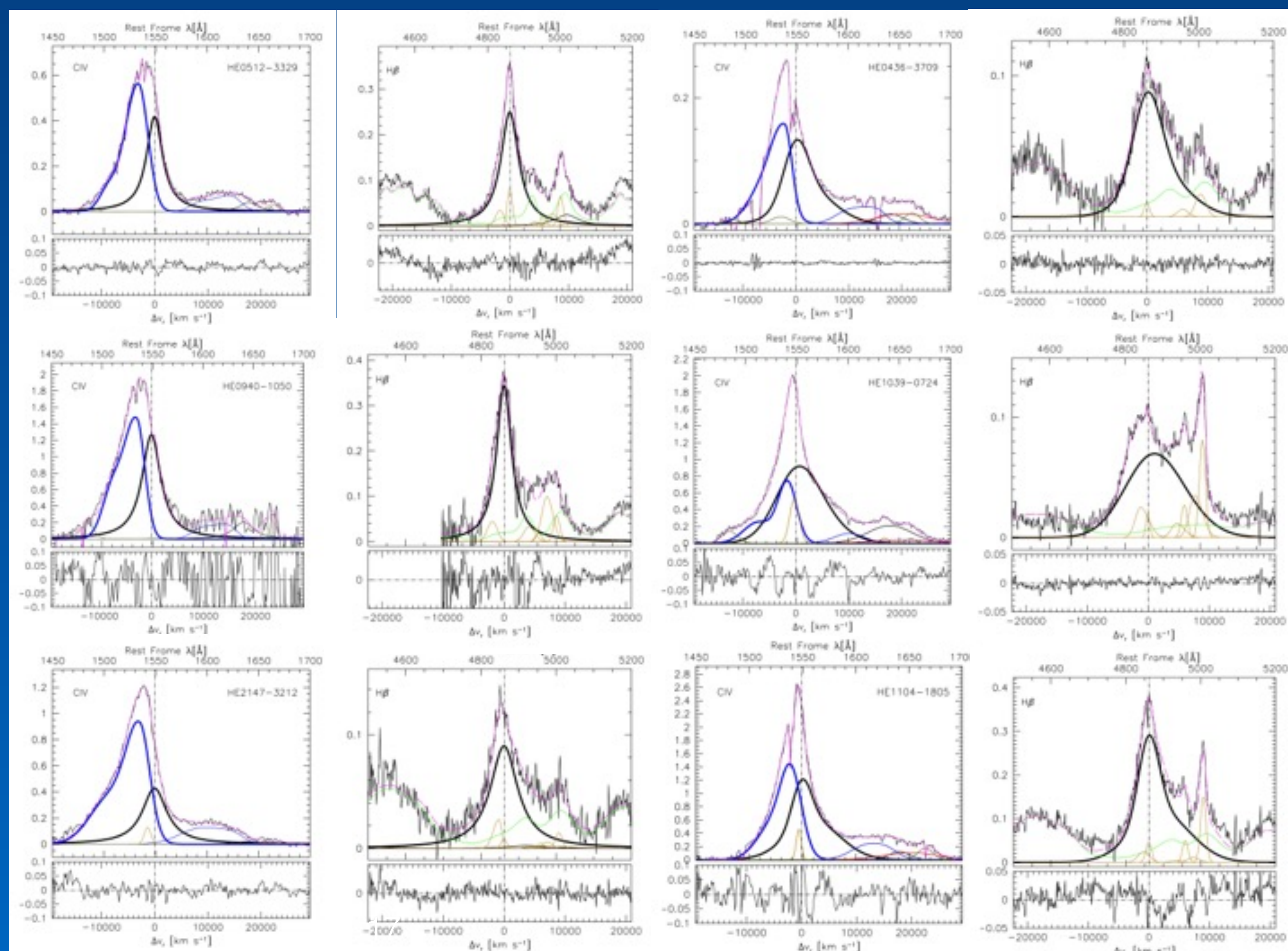

Virial broadening estimators: LIL Hβ at high-L

Higher luminosity implies a **displacement of the MS** toward larger FWHM(Hβ) i.e., larger masses

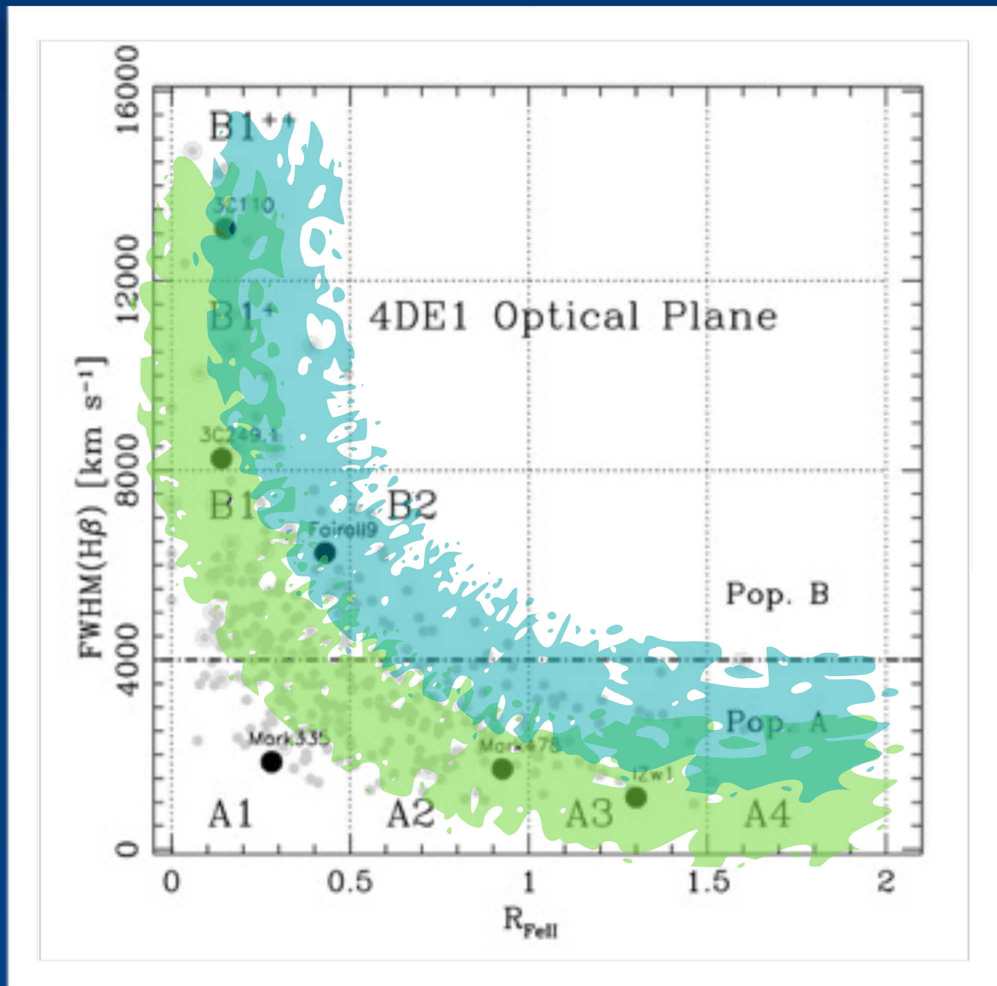

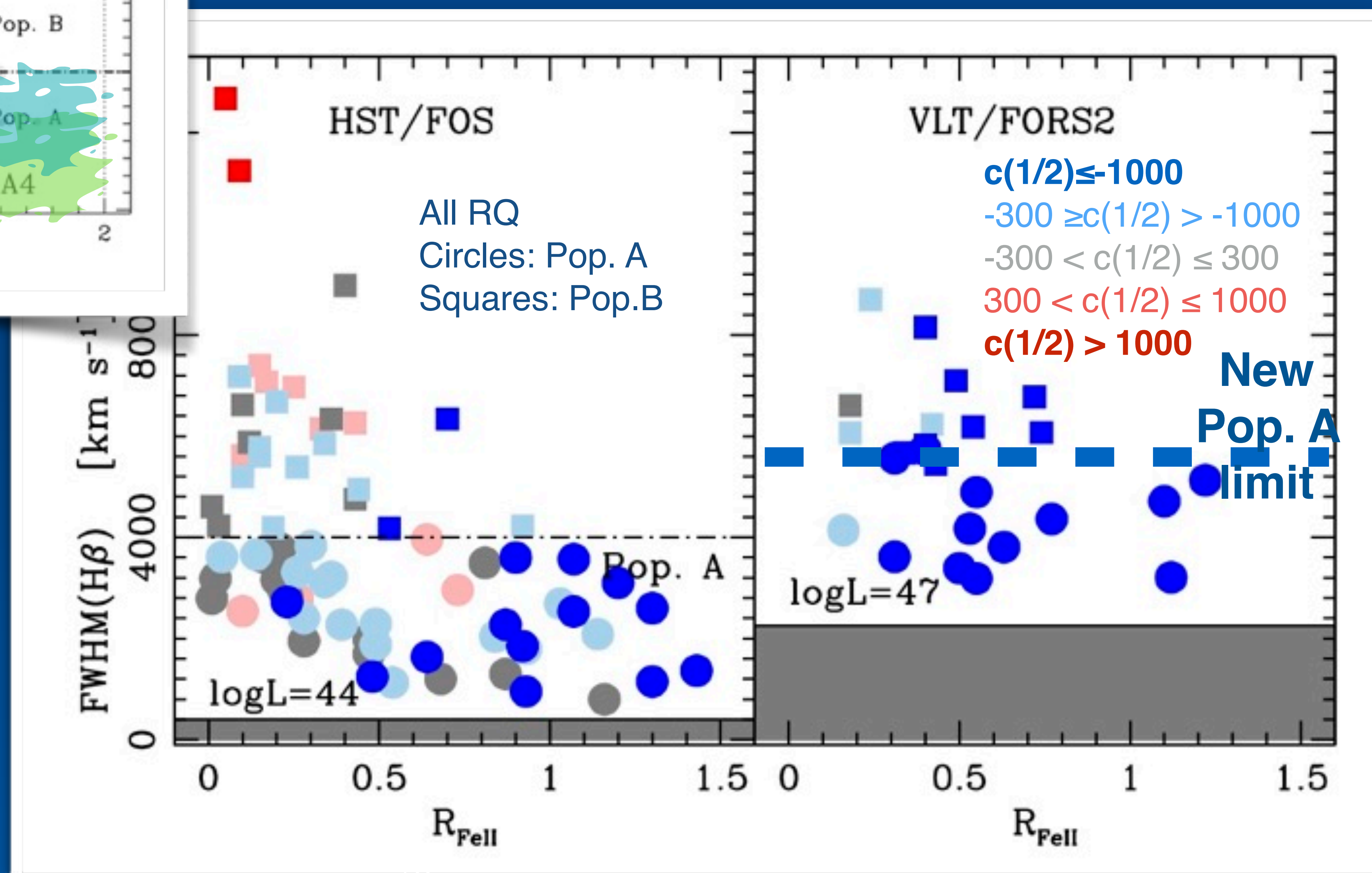

Sulentic et al., 2017

Virial broadening estimators: CIV vs Hβ FWHM

Low-L:
HST/FOS RQ sample of Sulentic et al.
2007 (CIV, 130 sources)
∩
Marziani et al. 2003 (Hβ, 215)
52 RQ sources

High-L:
VLT/FORS/ISAAC HE sample
28 objects

Same trends seen at low-z (≲1):
large FWHM CIV/ FWHM Hβ for Pop. A; rough consistency with large scatter for Pop. B

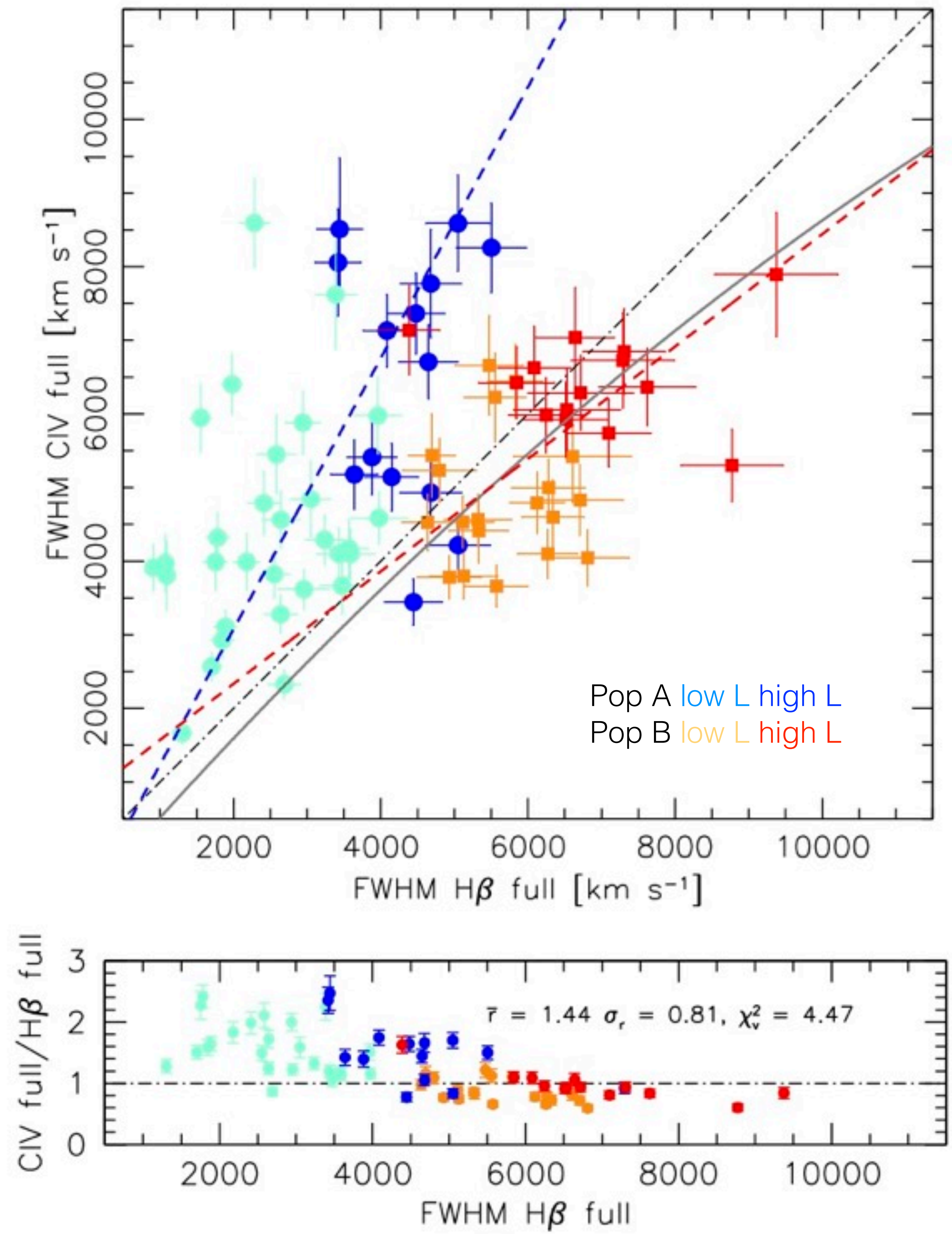

Virial broadening estimators: the HIL CIVλ1549

Correlation CIVλ1549 c(1/2) vs. FWHM

the HIL CIVλ1549 is broadened by a blueshifted excess

c(½) CIVλ1549

Increase in FWHM(CIVλ1549) associated with a blueshifted component

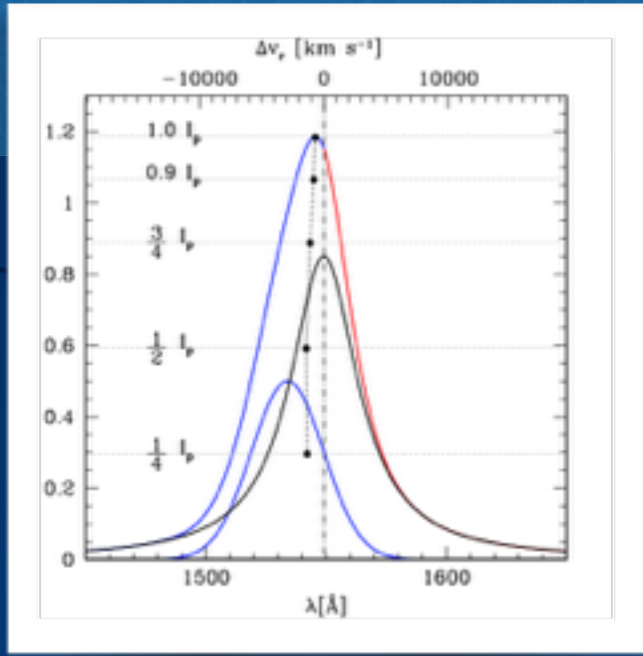

low *z* sample UV FOS data (130) +HE high L sample (28, red)

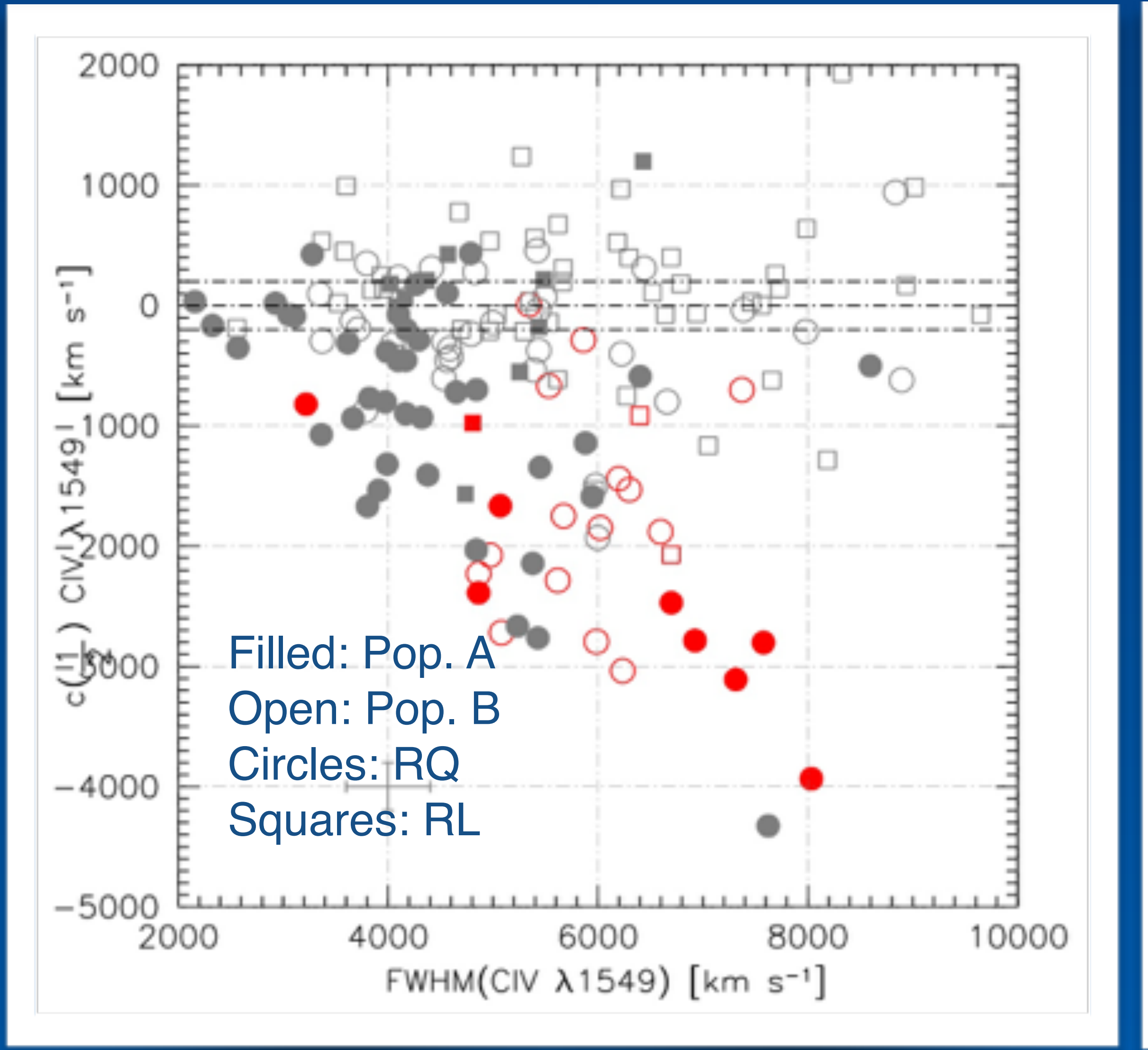

Pop. A RQ only

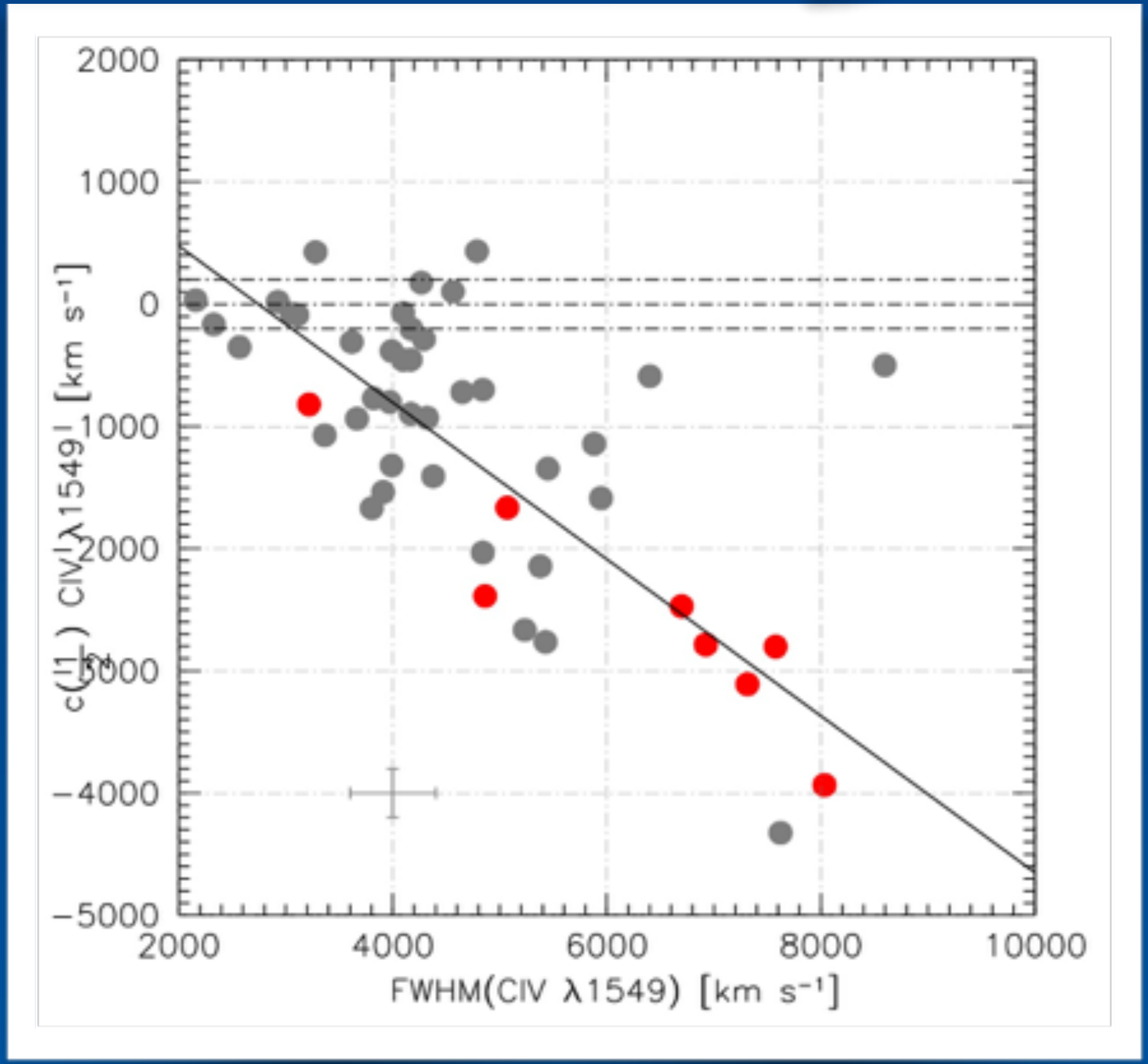

Coatman et al. 2017; Sulentic et al. 2017, Sulentic et al. 2007

Worrisome implications for M_{BH} estimates from CIVλ1549 FWHM

Virial broadening estimators: HIL CIV corrections

Scaling law that assumes $M_{BH} \propto FWHM^{0.5}$: accounts for the over-broadening of Pop. A sources, but overcorrects for Pop. B.

Correction dependent on L/L_{Edd} or a proxy such as the SiIV+OIV]1400 blend/CIV 1549 ratio: interesting, but not working well on our sample, especially for Pop. B.

Empirical correction based on CIV blueshift: works fairly well for high L sources *only.* Still Requires knowledge of the rest frame.

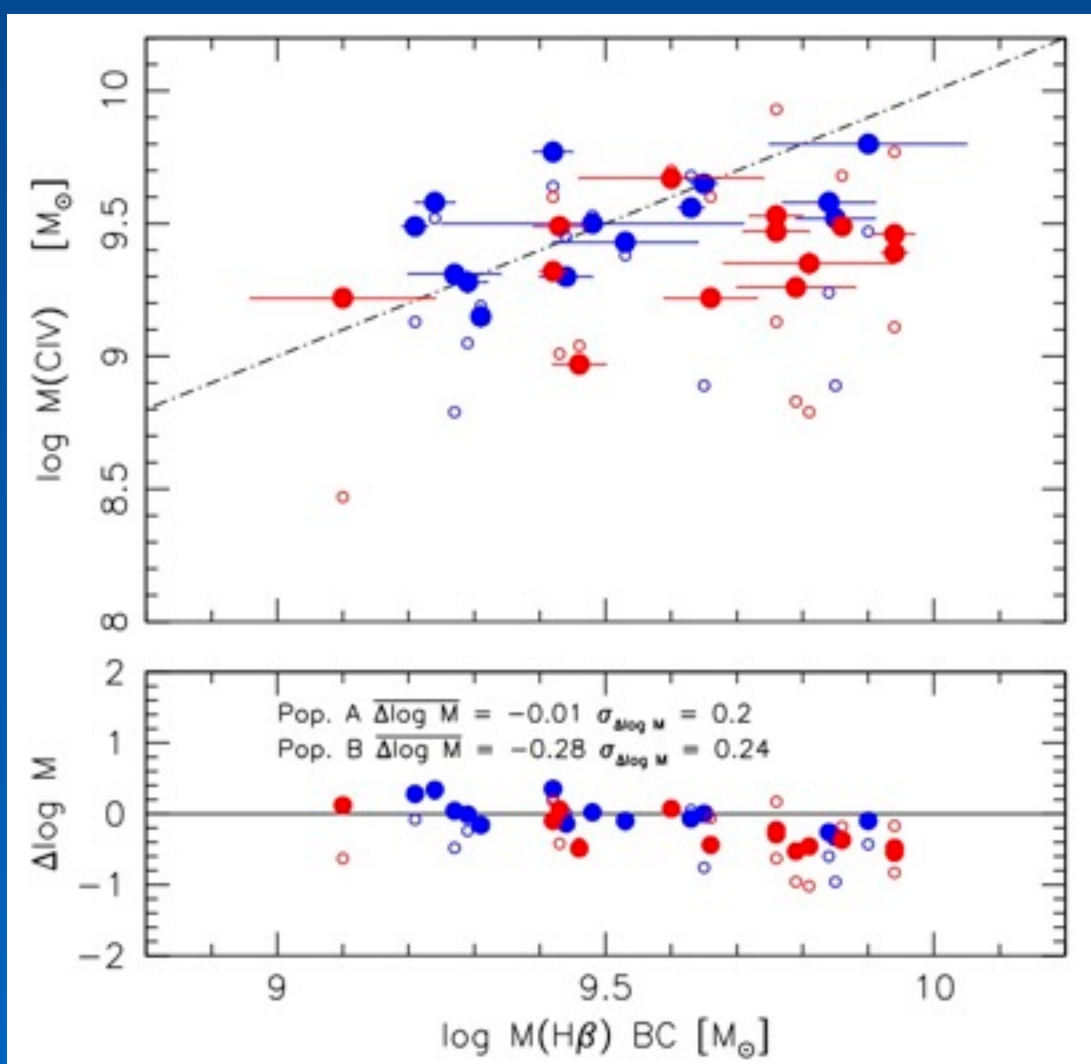

Shen & Liu 2012; Park et al. 2013; Coatman et al. 2016; 2017; Brotherton et al. 2015

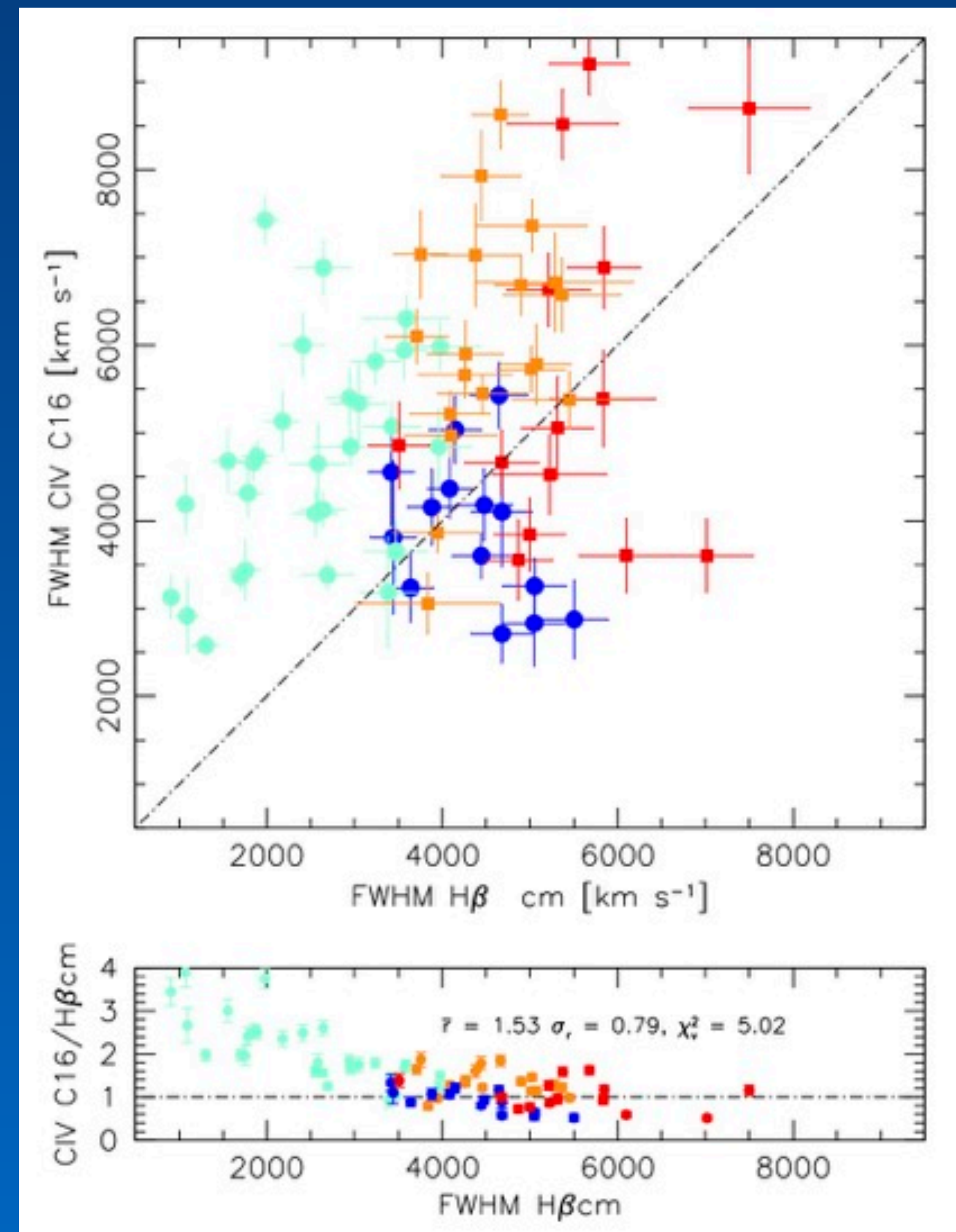

Virial broadening estimators: HIL CIV corrections

A threshold in CIV *shift amplitude (c(1/2))* and *L/L_{Edd}* at *$L/L_{Edd} \approx 0.2$*

Strong correlation with *L/L_{Edd}* if blueshifts are significant (bottom panels)

Weak but significant correlation with luminosity: partial CC c(1/2) — L (L/L_{Edd} hidden) significant at about 2σ

Multivariate analysis confirms dependence on both L and L/L_{Edd}.

Blueshift trends are consistent with a radiation-driven outflow

$$v_{term} \propto v_K \sqrt{\mu \frac{L}{L_{Edd}}} \propto L^{-a/2} M_{BH}^{1/2} \sqrt{\mu \frac{L}{L_{Edd}}}$$

$$\propto L^b \sqrt{\frac{L}{L_{Edd}}} \quad if \quad L^{-a/2} M_{BH}{}^{1/2} \mu^{1/2} \propto L^b$$

where v_K is the Keplerian velocity and μ is the force multiplier; Laor & Brandt 2002

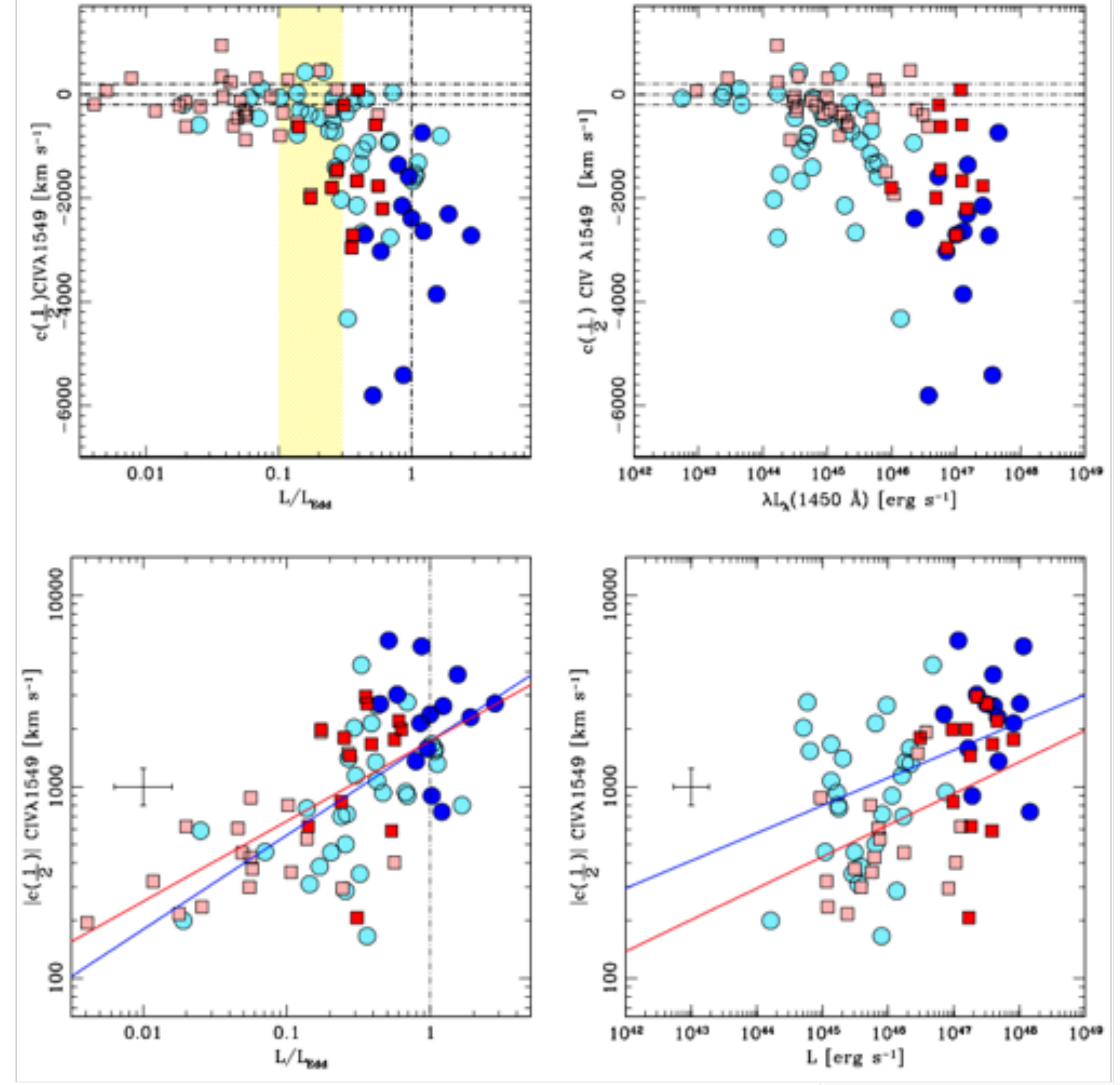

Circles: Pop. A
Squares: Pop. B

A pure dependence on L arises for L/L_{Edd} in a small range.
A strong dependence on L/L_{Edd} and a weak dependence on L can be achieved under a variety of scenarios; strength and form of L and L/L_{Edd} are sample dependent.

Sulentic et al., 2017

Virial broadening estimators: HIL CIV corrections

A correction based on L and c(1/2) reduces scatter, but coefficients are different for Pops. A and B.

as ξ_{CIV} =FWHM(Hβ_{BC})/FWHM(CIVλ1549), then

$$\xi_{\mathrm{CIV}} = \frac{1}{\beta\left(\alpha - \log \lambda L_{\lambda}(1450)\right)\cdot\left(\left|\frac{c(\frac{1}{2})}{1000}\right|\right) + \gamma}$$

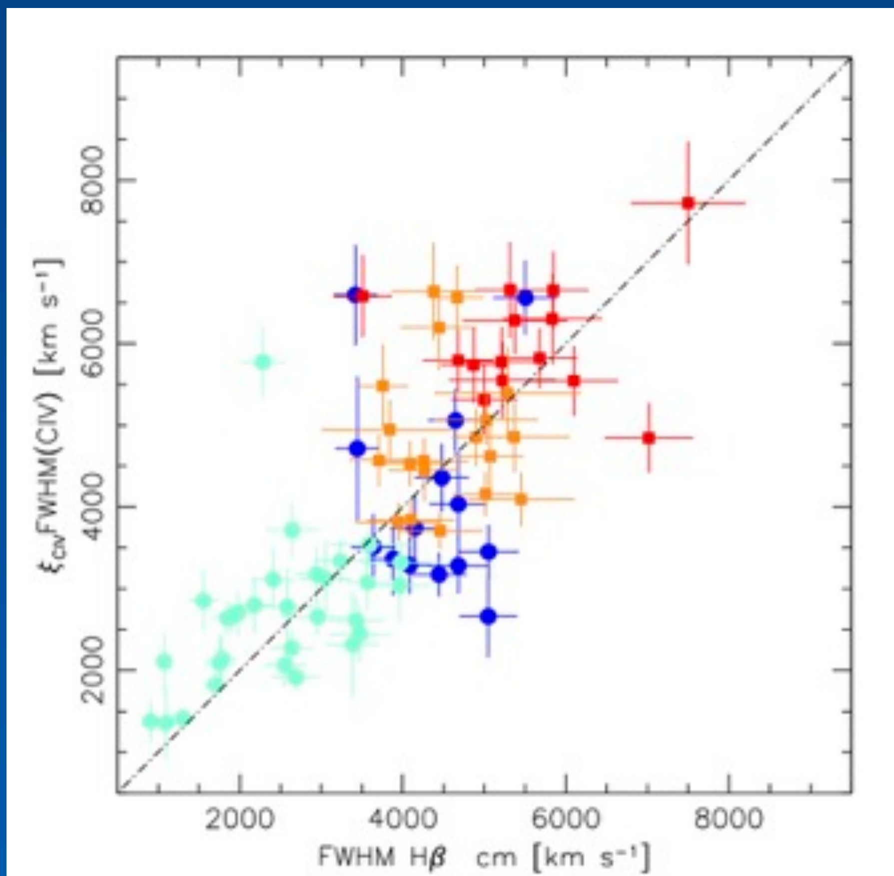

α ≈ −0.347 ± 0.148, β ≈ −0.335 ± 0.083, γ ≈ 1.087 ± 0.09 for Pop. A

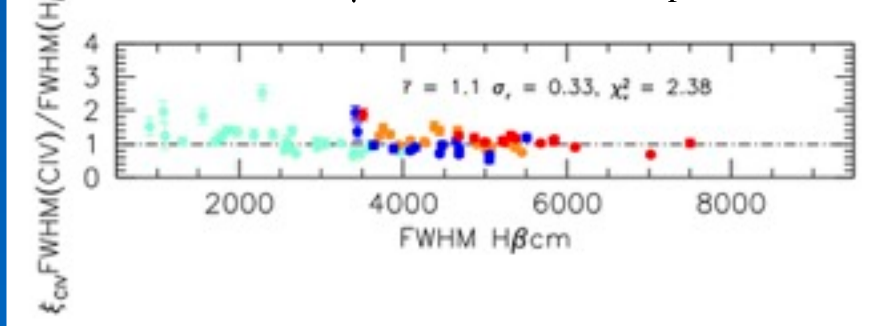

For Pop. B the correction is highly uncertain. A larger sample of Pop. B is needed.

Corrections based on c(1/2) require rest-frame knowledge.

A theoretical correction requires that c(1/2) CIV and ionization conditions are accounted for.

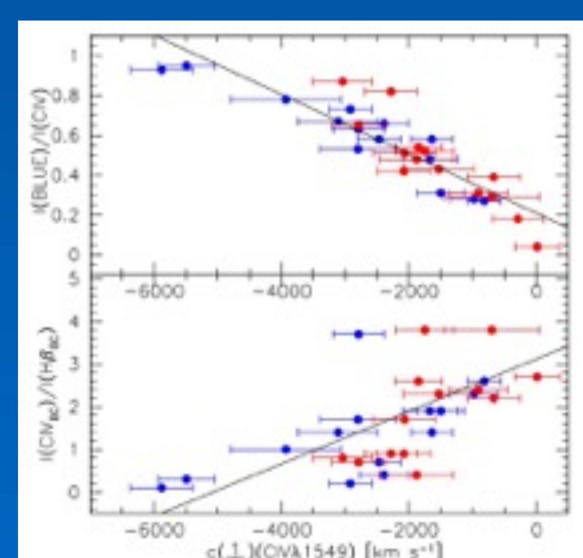

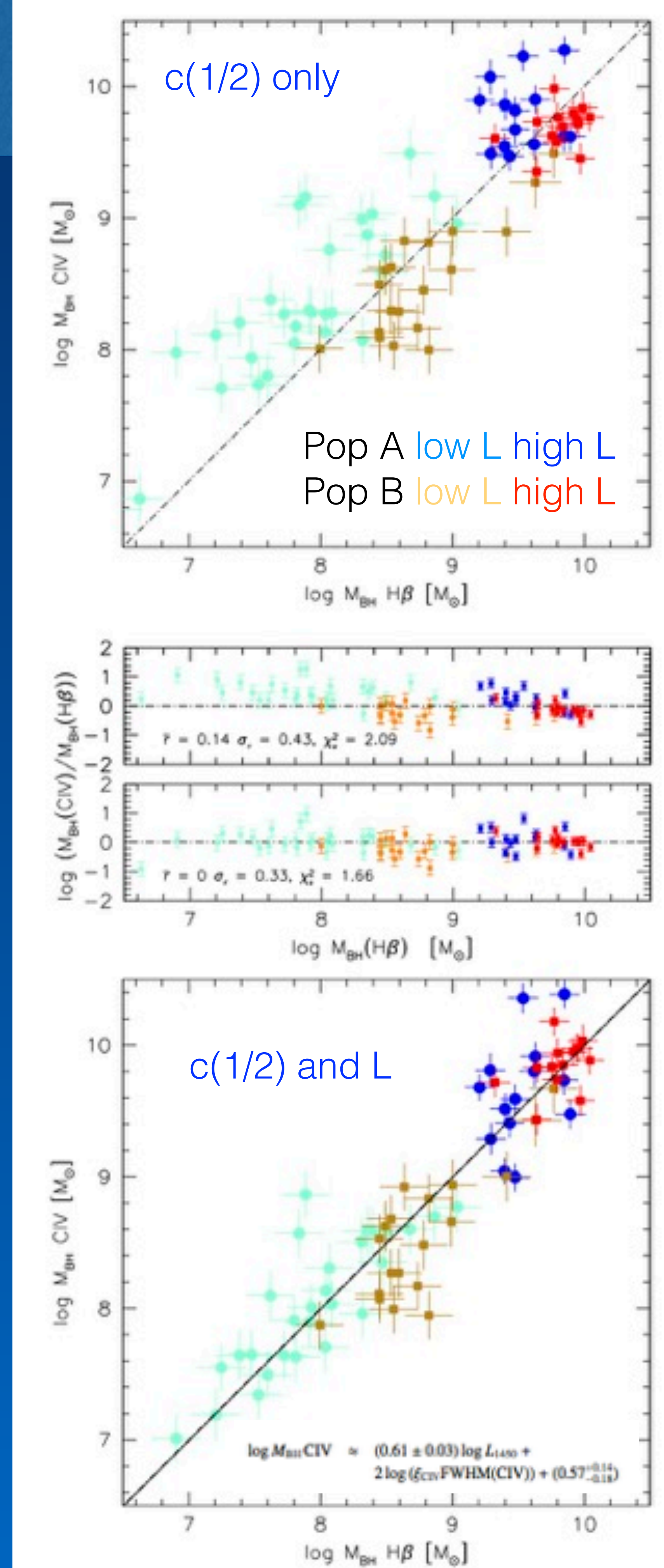

Virial broadening estimators: HIL CIV corrections —The "Eddington ratio bias"

Sulentic et al. 2015

Selection effects on L/L_{Edd} in flux limited samples

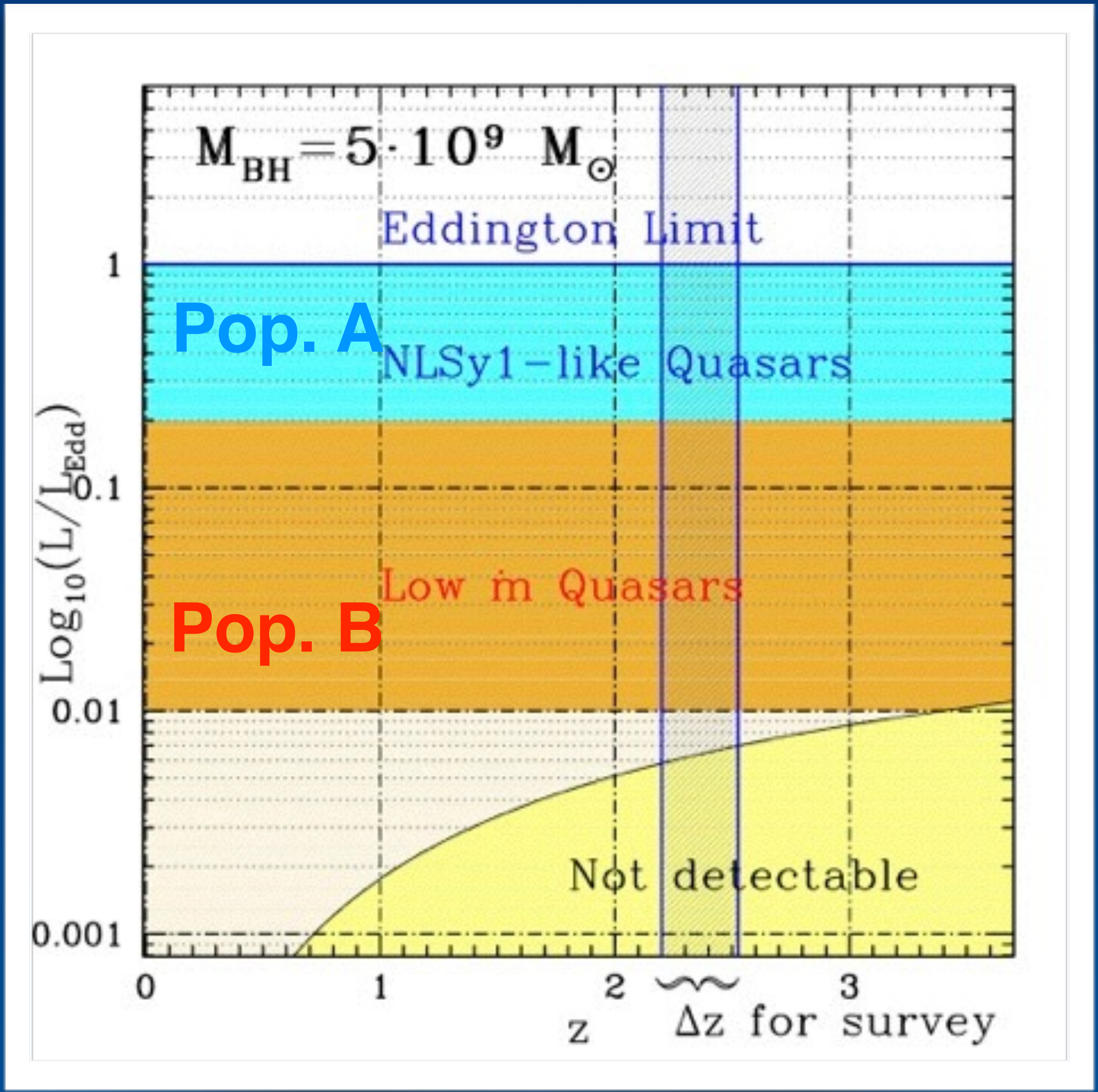

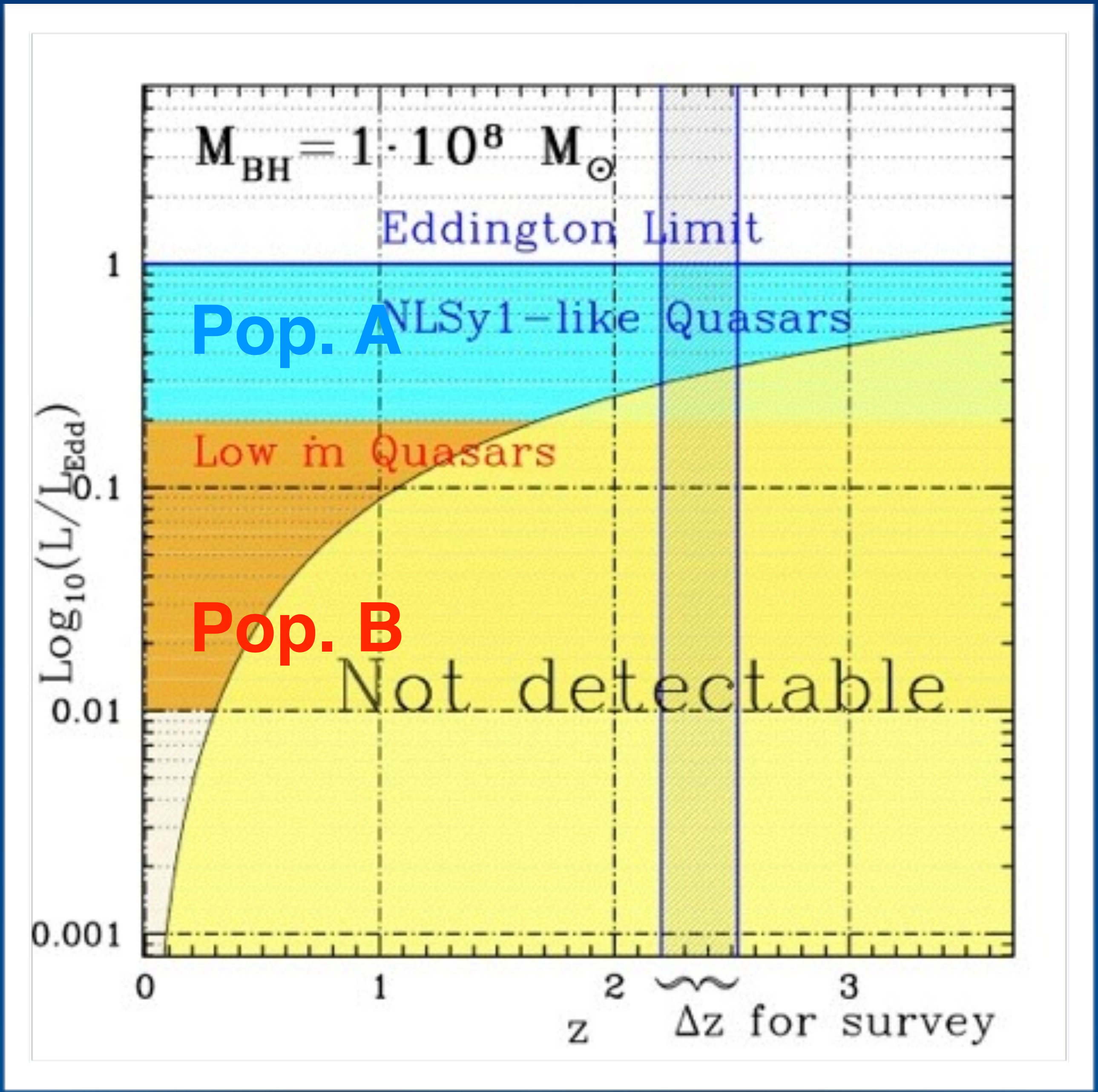

Higher L/L_{Edd} selected at higher *z:* the high frequency of CIV blueshifts associated with an "Eddington ratio" bias.

***L/L_{Edd}* (using c(1/2) as a proxy) and *L*-based corrections may remain sample dependent.**

Virial broadening estimators from IILs: the 1900 Å blend

CIII] measurements have serious problems:
in Pop. A; CIII] faint, blended with FeIII
in Pop. B: affected by VBC.

FWHM AlIIIλ1860 = FWHM SiIII]λ1892

Table 1
Line Components in the λ1900 Blend

Ion	λ	χ	$E_l - E_u$	Transition	A_{ki}	n_c
	(Å)	(eV)	(eV)		(s^{-1})	(cm^{-3})
(1)	(2)	(3)	(4)	(5)	(6)	(7)
Si II	1808.00	8.15	0.000–6.857	$^2D^o_{3/2} \rightarrow {}^2P_{1/2}$	2.54×10^6	...
Si II	1816.92	8.15	0.036–6.859	$^2D^o_{5/2} \rightarrow {}^2P_{3/2}$	2.65×10^6	...
Al III	1854.716	18.83	0.000–6.685	$^2P^o_{3/2} \rightarrow {}^2S_{1/2}$	5.40×10^8	...
Al III	1862.790	18.83	0.000–6.656	$^2P^o_{1/2} \rightarrow {}^2S_{1/2}$	5.33×10^8	...
[Si III]	1882.7	16.34	0.000–6.585	$^3P^o_2 \rightarrow {}^1S_0$	0.012	6.4×10^4
Si III]	1892.03	16.34	0.000–6.553	$^3P^o_1 \rightarrow {}^1S_0$	16700	2.1×10^{11}
[C III]	1906.7	24.38	0.000–6.502	$^3P^o_2 \rightarrow {}^1S_0$	0.0052	7.7×10^4
C III]	1908.734	24.38	0.000–6.495	$^3P^o_1 \rightarrow {}^1S_0$	114	1.4×10^{10}
Fe III	1914.066	16.18	3.727–10.200	$z^7P^o_3 \rightarrow a^7S_3$	6.6×10^8	...

FWHM AlIII (anchored to FWHM SiIII]) provides a virial broadening estimator (but AlIII is a resonant line).

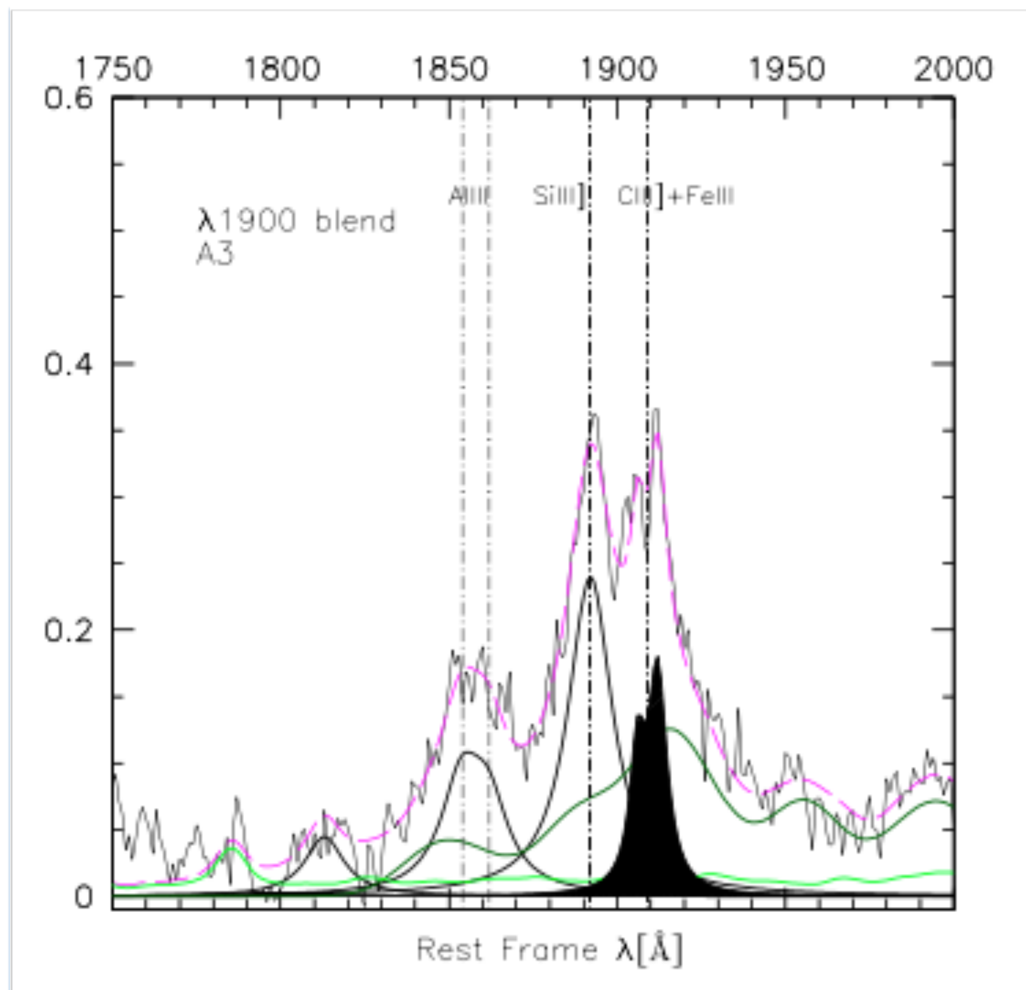

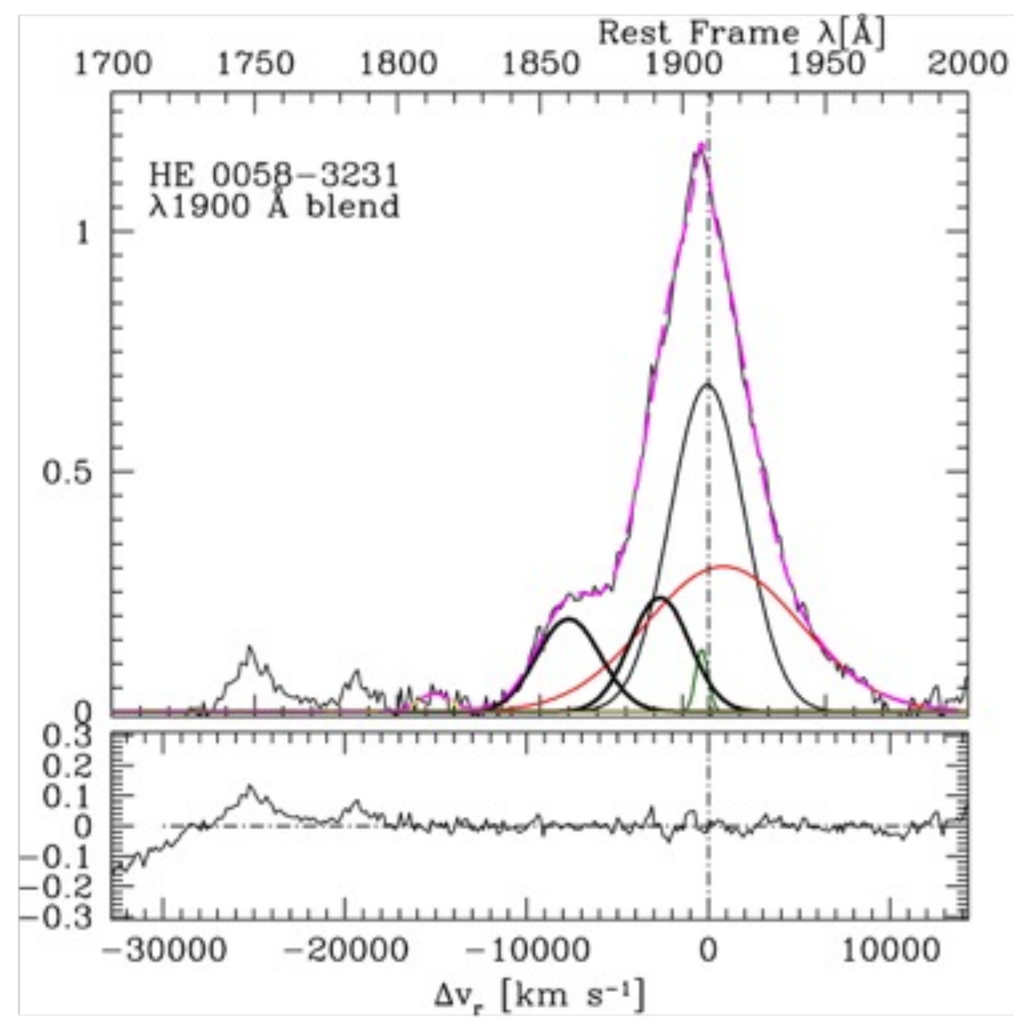

Virial broadening estimators from IILs: the 1900 Å blend

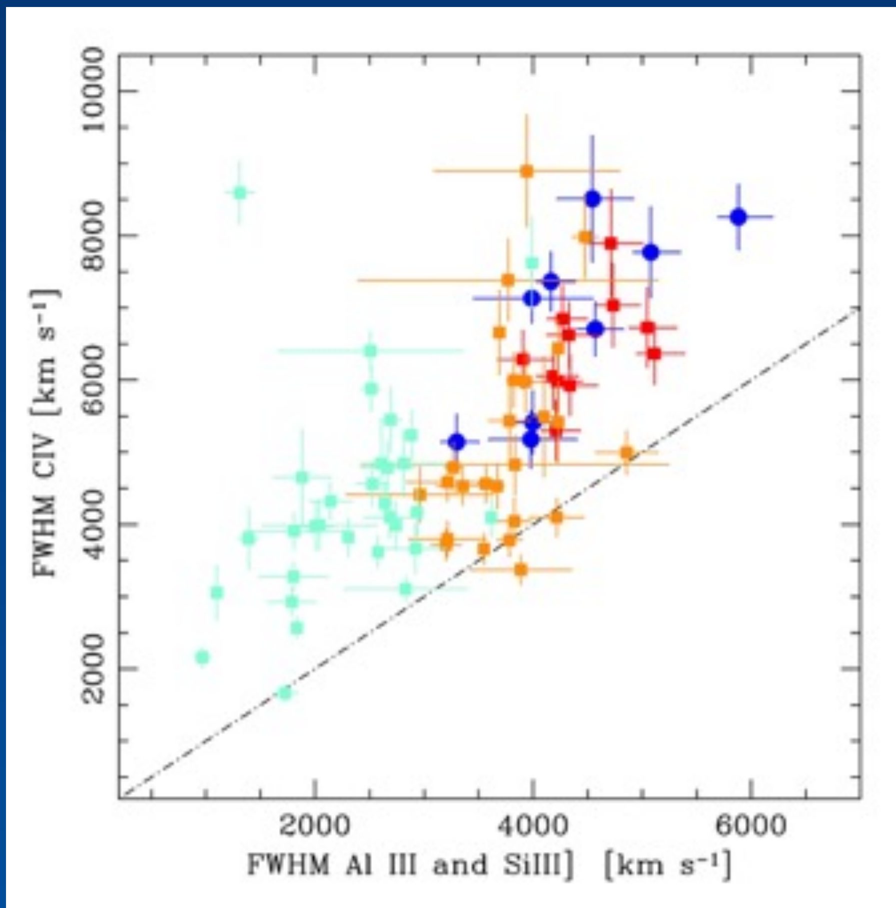

AlIII - SiIII] narrower than CIV, but no clear trend

AlIII shifts < 0.2 CIV shifts; profile is symmetric and (almost) unshifted in most sources.

AlIII - SiIII] relation to CIII]: AlIII broader, but with large scatter

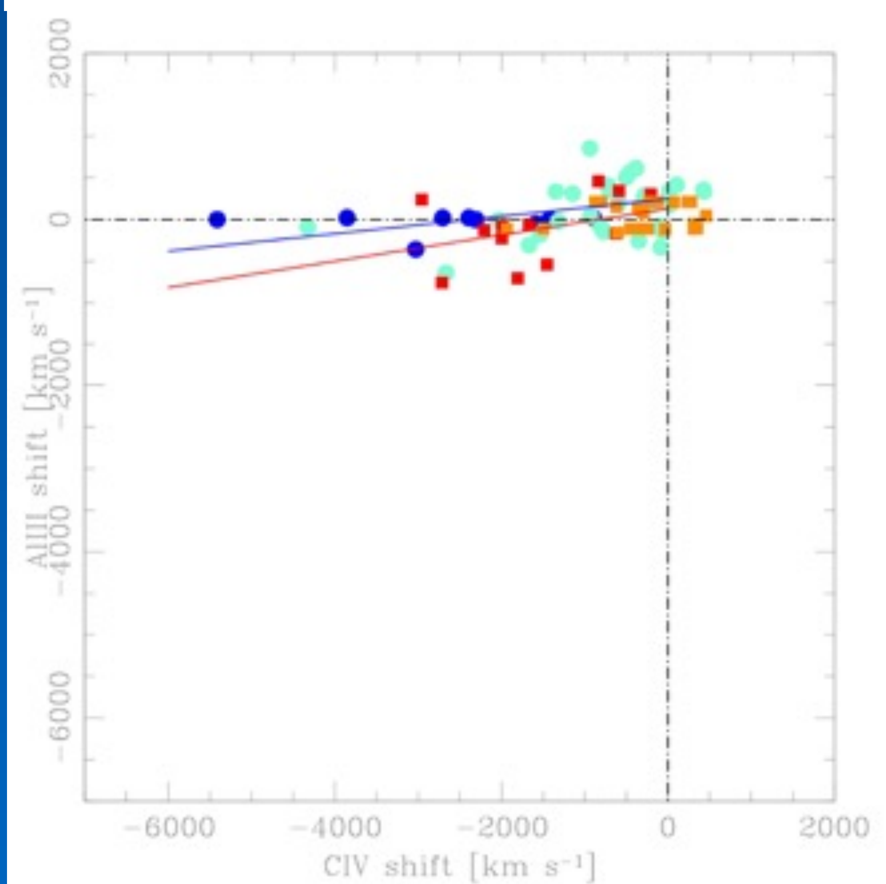

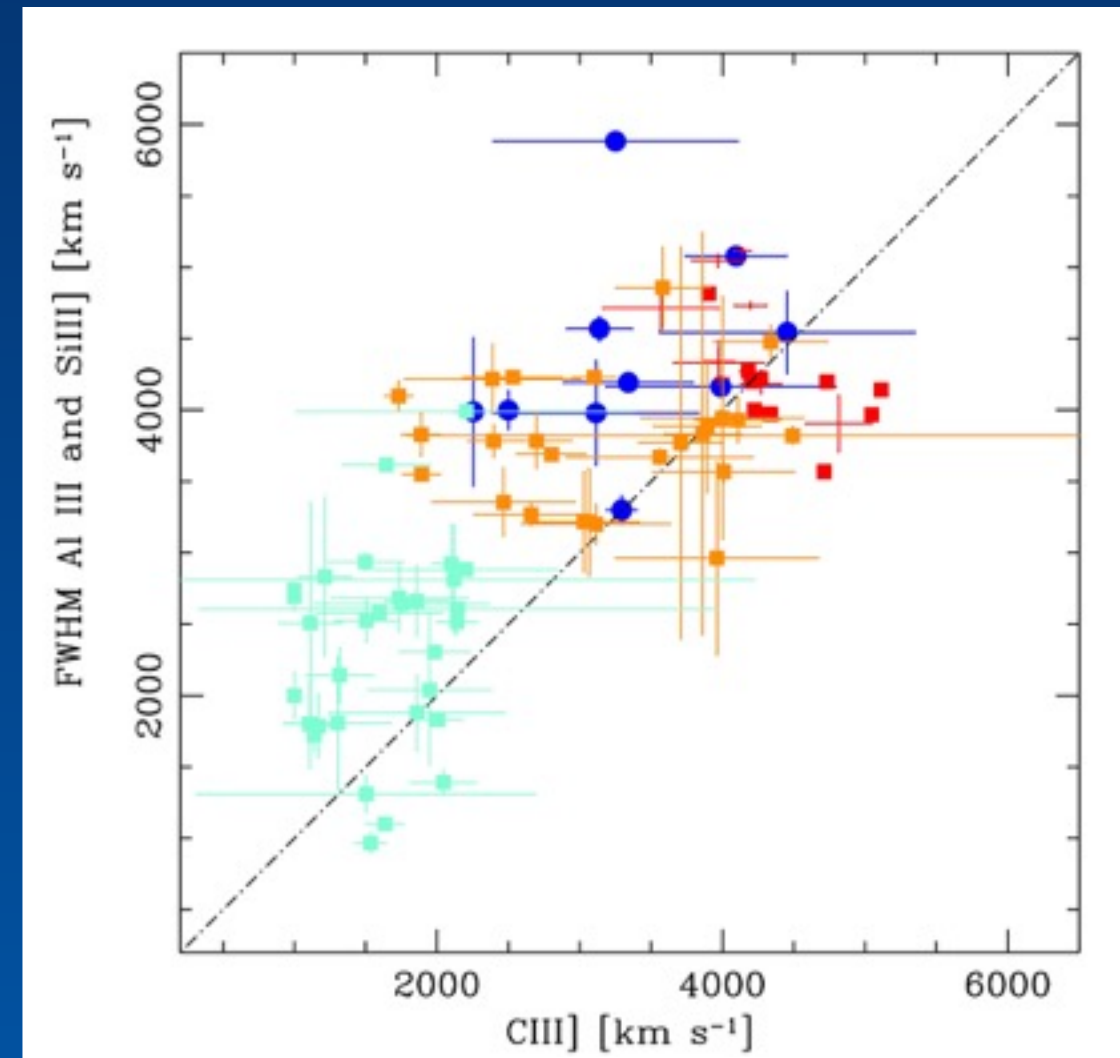

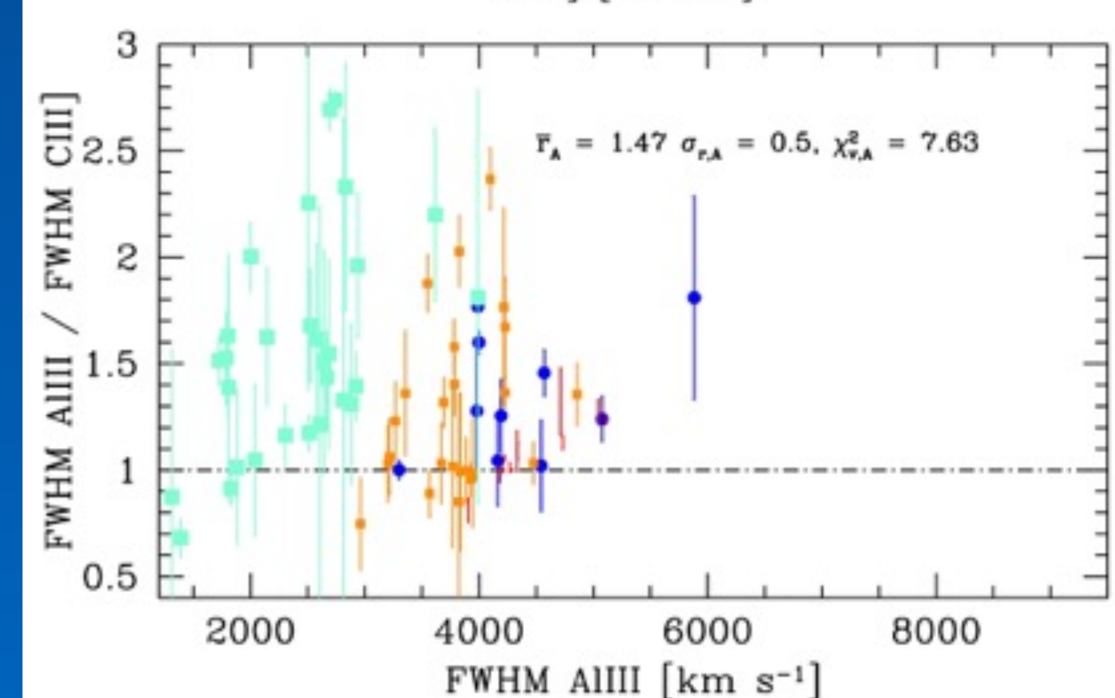

Virial broadening estimators from IILs: the 1900 Å blend

Pop. A: very good agreement with Hβ:
ξ_{AlIII} = 1.0 (Pop. A)

Pop. B: lines are narrower than Hβ:
ξ_{AlIII} = 1.35 (Pop. B)
$FWHM_{vir}$ = FWHM $H\beta_{BC}$ = 1.35 FWHM $_{AlIII}$

VBC/BC decomposition choices
creating a small bias

3VBC: med 0.97 SIQR 0.14;
NOVBC (wrong) med 1.05 SIQR 0.13

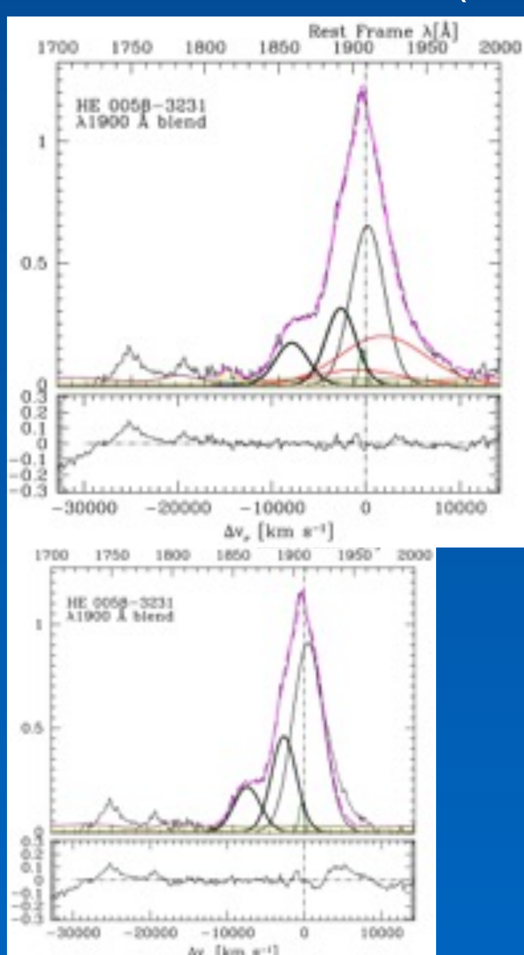

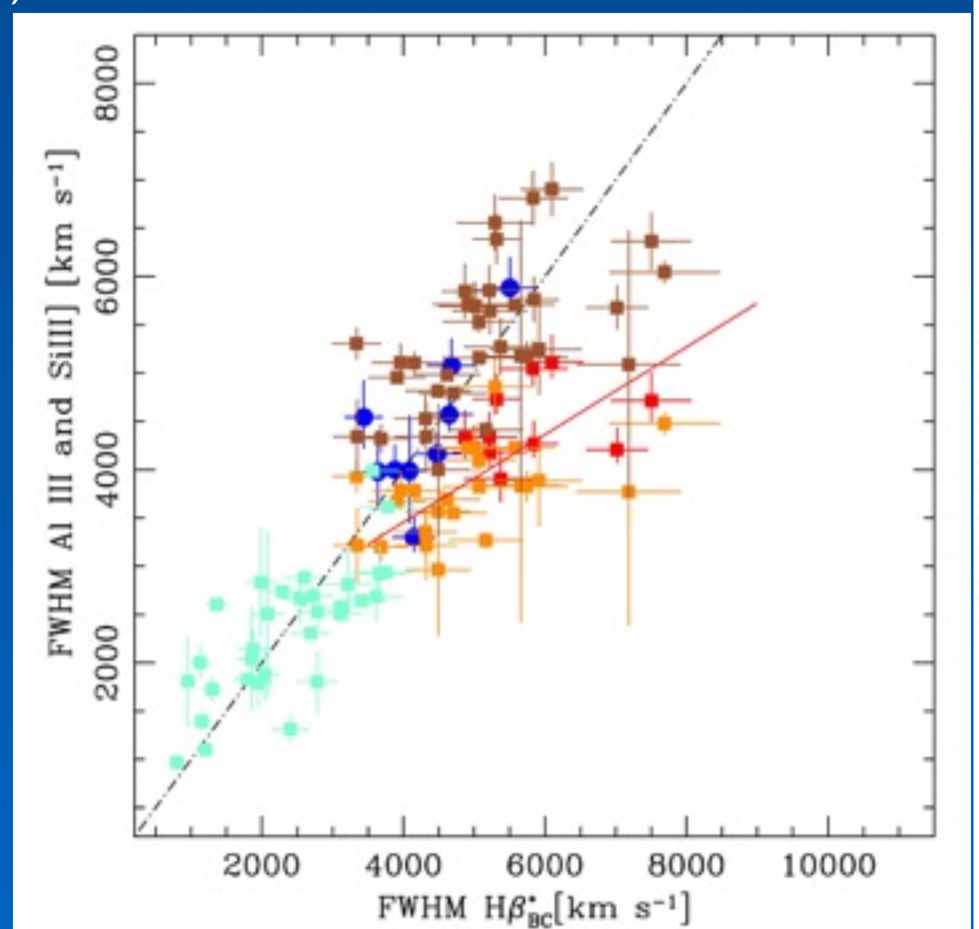

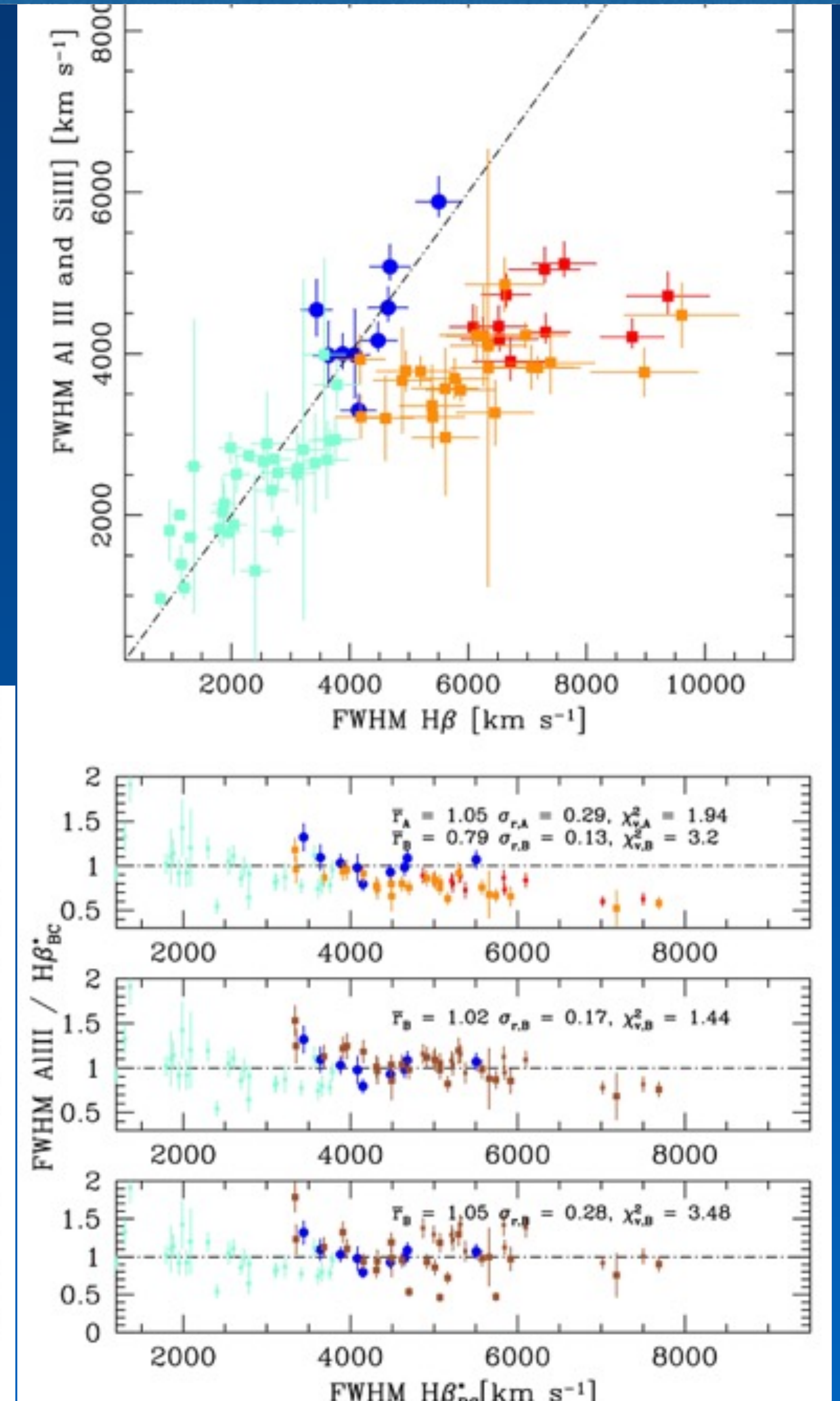

“Photoioionization” Masses

$$U = \frac{\int_{\nu_0}^{+\infty} \frac{L_\nu}{h\nu} d\nu}{4\pi r_{\rm BLR}^2 n_{\rm e} c}$$

$$r_{\rm BLR} = \left(\frac{\int_{\nu_0}^{+\infty} \frac{L_\nu}{h\nu} d\nu}{4\pi U n_{\rm e} c} \right)^{\frac{1}{2}}$$

$$r_{\rm BLR} = \underbrace{\frac{1}{(4\pi c)^{\frac{1}{2}}}}_{\rm const.} \underbrace{(U n_{\rm e})^{-\frac{1}{2}}}_{\rm diagnostics} \left(\underbrace{\int_{\nu_0}^{+\infty} \frac{L_\nu}{h\nu} d\nu}_{\#\ \rm ionizing\ \ photons} \right)^{\frac{1}{2}}$$

The photon flux $Un_{\rm e}$ is estimated using diagnostic ratios involving AlIII 1860, SiIII] 1892, SiII 1816, CIV 1549, SiIV +OIV] 1400

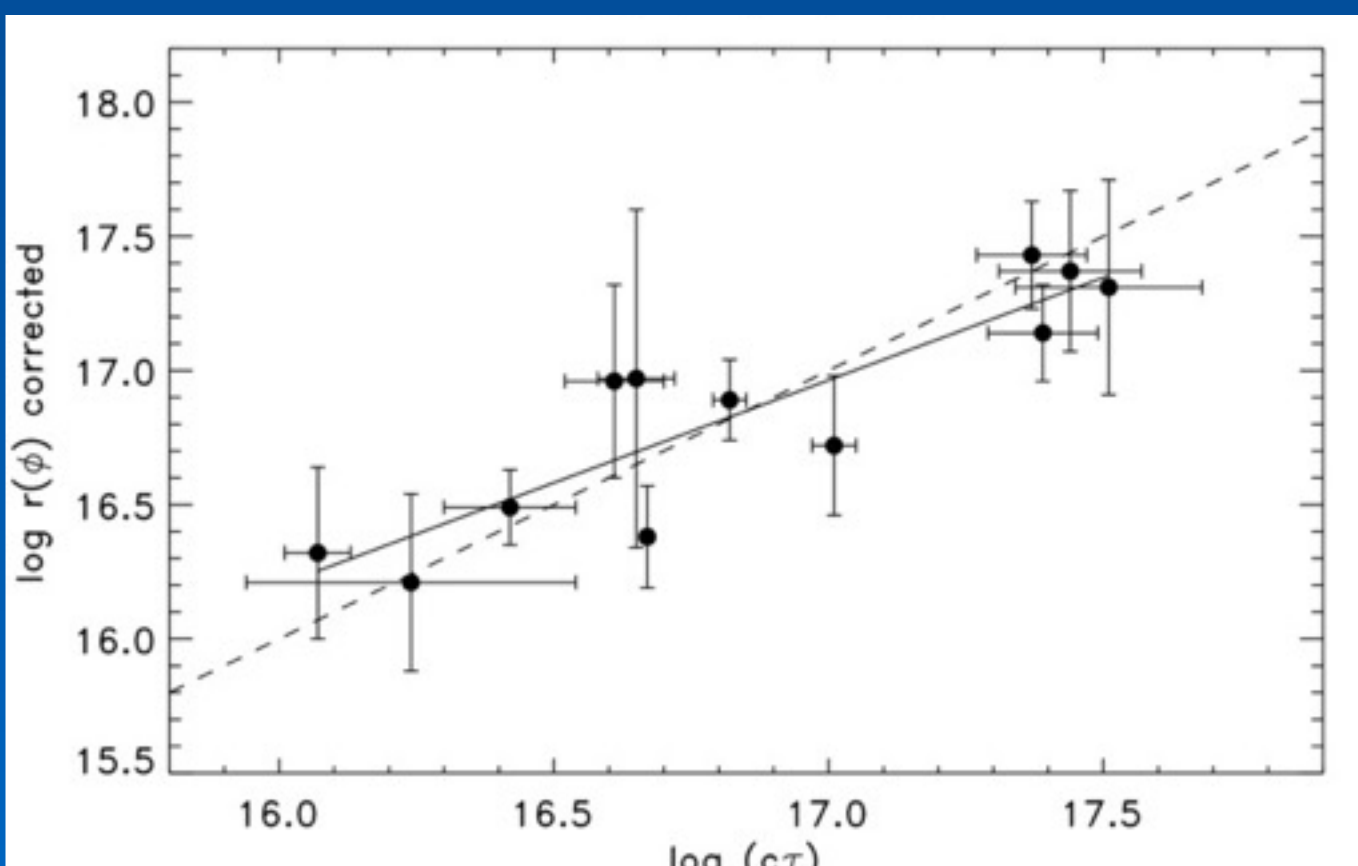

$r_{\rm BLR}$ estimates from photo-ionization agree with cτ from RM

(sample of 12 sources, Negrete et al. 2013)

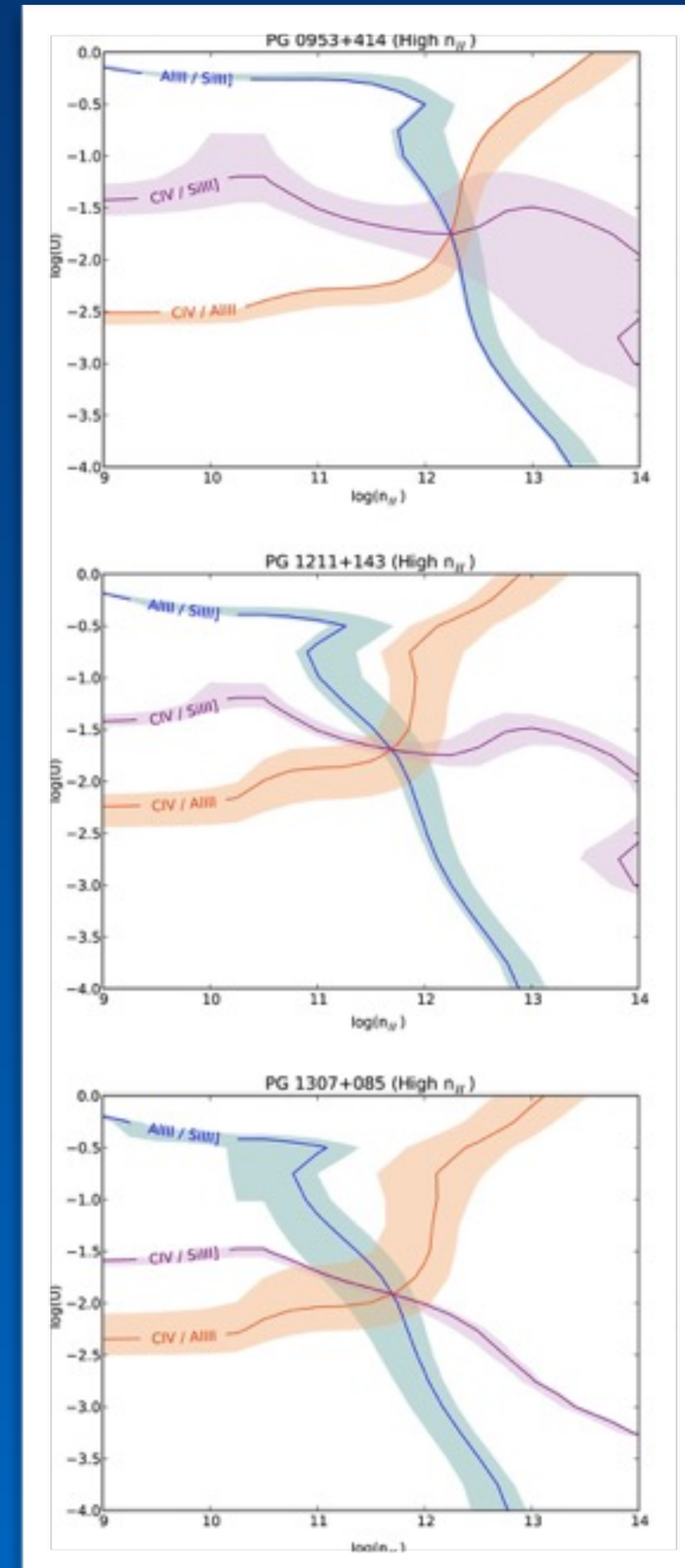

The photoionization method provides an unbiased estimator of r_{BLR}

Both r_{BLR} and M_{BH} estimates at high L remains largely untested

Collin et al. 2006

	f(σ_line)	df(σ_line)	f(FWHM)	df(FWHM)
	MEAN SPECTRUM			
total	3.85	1.15	1.17	0.50
Pop1	4.20	2.09	1.81	1.38
Pop2	3.48	1.09	0.69	0.19
PopA	3.93	1.97	2.12	1.47
PopB	3.75	1.13	0.52	0.13

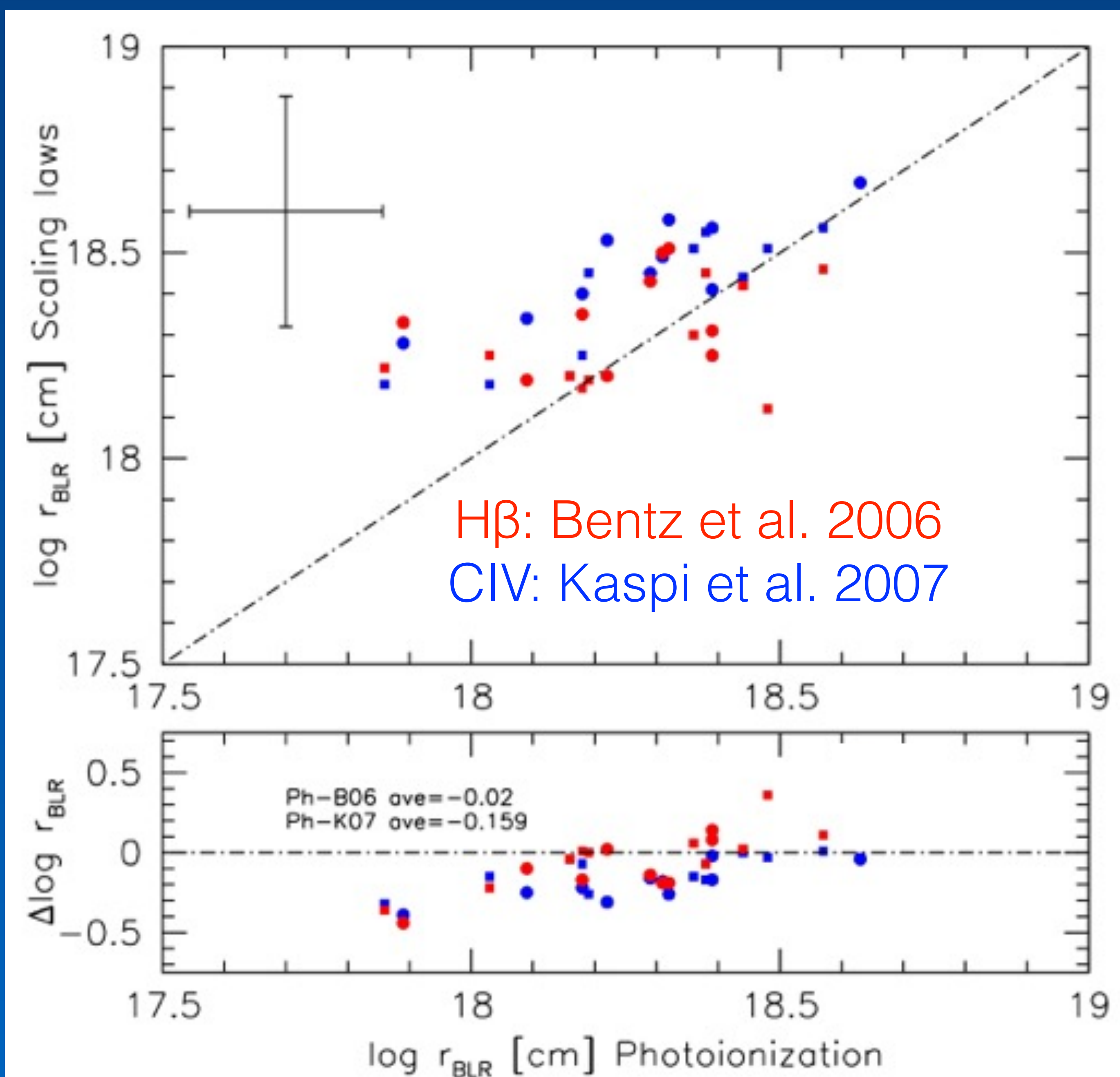

f =1 or different f: which is right? We do not know.

M_{BH}: the bias emphasizes the role of f

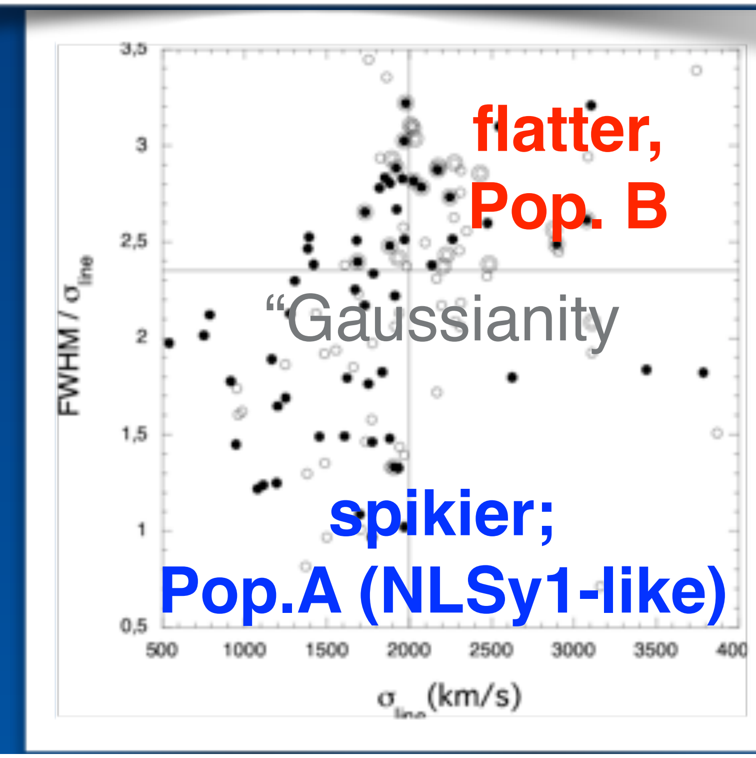

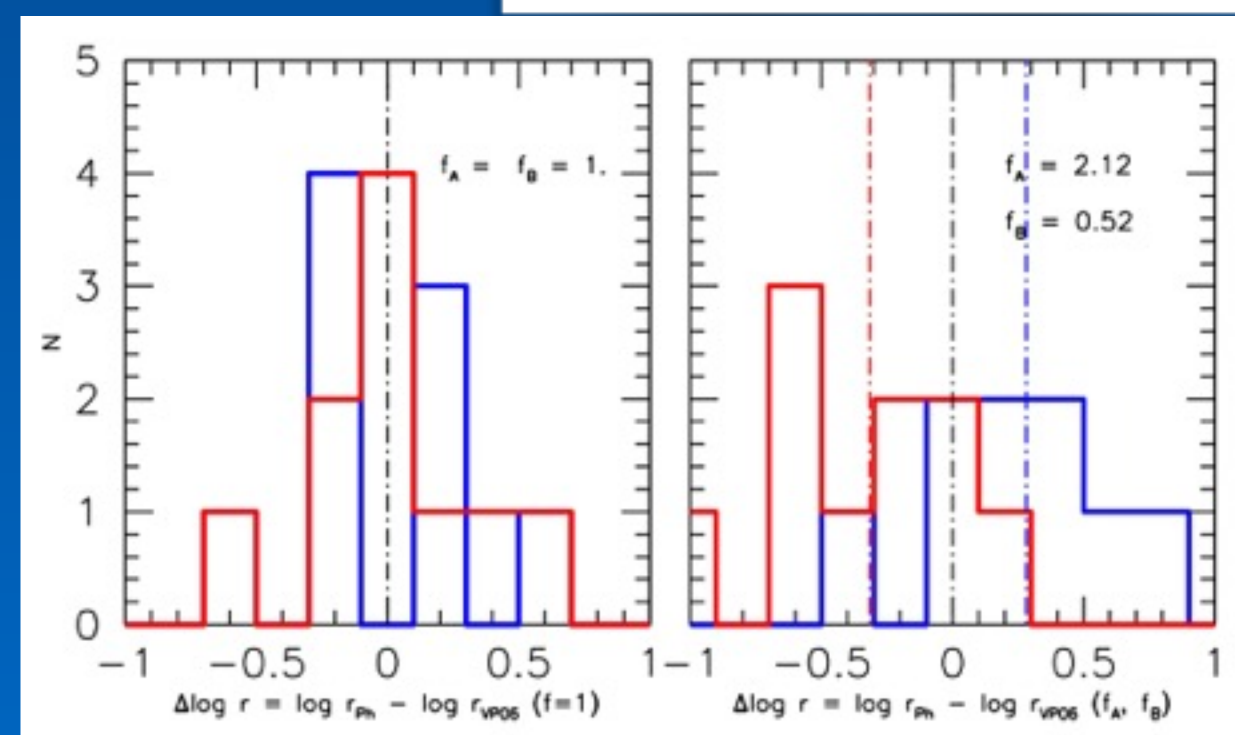

Conclusion

Low-ionization lines (Hβ, MgIIλ2800) provide reliable virial broadening estimators by applying corrections to the observed line width. The corrections depend on the spectral type along the E1 MS, but they are relatively small (less than 20%), and work up to the highest L of quasars.

The **HIL CIVλ1549 is not immediately providing a reliable virial broadening estimator.** The profile is broadened by an excess emission on its blue side. The shift amplitude depends on both L/L_{Edd}, and L. Large shifts are observed in Pop. A, with Eddington ratio above a critical $L/L_{Edd} \sim 0.2$.

Corrections applied to the observed CIV broadening remain cumbersome even for Pop. A. Pop. B sources at low Eddington ratio require a different correction (ill defined by the present analysis). They require rest frame determination.

Preliminary result on the 1900 blend indicate that the **IILs lines could provide a better virial broadening estimator than CIV**, even if more data are needed to assess their reliability.

The solution may be to abandon scaling laws altogether and to attempt M_{BH} estimates on an individual basis, considering r_{BLR} from photoionization and $f=f(L/L_{Edd}, a, \theta)$ along the E1 sequence.